



Democratic and Popular Republic of Algeria
Ministry of Higher Education and Scientific Research



Amar Thelidji-Laghouat University

FACULTY: TECHNOLOGY

DEPARTMENT: Electronics

MASTER'S THESIS

Presented by: CHEKNAR Zeyneb

FIELD: Science and Technology

COURSE: Electronics

OPTION: Electronics of embedded systems

Theme

**Back stepping Control for Optimal Energy Management
in Renewable Energy Systems:
Fuel Cell-Based Approach**

Defense jury:

Name and First Name	Grade	Quality
RahmaniAbdallah	MC-B	President
RougabIlyas	MC-B	Examineur
SilaaMohammed Yousri	MC-B	Encadreur

Promotion :2024

بِسْمِ اللَّهِ الرَّحْمَنِ الرَّحِيمِ
وَأَنْ لَّيْسَ لِلْإِنْسَانِ إِلَّا مَا سَعَى
وَأَنْ سَعْيُهُ سَوْفَ يُرَى
صدق الله العظيم

الاهداء

الى من عاش فينا قبل ان نعيش فيه وعرفناه في دفاتر التضحيات ووطننا الثاني
فلسطين قبلتنا الاولى ومسرى حبيبنا ونبينا الكريم جمعنا الله في اقصانا فاتحين
مهللين مكبرين وليس ذلك على الله بعسير إلى بلد المليون ونصف شهيد، الجزائر
العظيمة، أهديك من القلب ألف تحية وسلام

مثل كل البدايات الا بتسييره وما بلغنا النهاية الا بتوفيقه وماحققنا المراد الا
بفضله فالحمد لله الذي وفقني لاتمام هذه الخطوة في مسيرتي الدراسية
الى سندي وقوتي ومهجتي وبلسم جراحي الى من كان دعاءها سر نجاحي وضوء
املي في ظلام الياس الى ملاذي وركن الذي لايميل امي العزيزة "حليمة" دمتي
قوتي وفخري في هذه الحياة

الى من احمل اسمه بكل فخر الى مامني سيد قلبي من فرش لي ورود النجاح
وسار على الاشواك زميلي ومعلمي الاول ابي "العرج"
الى اخوتي الذين تقاسمت معهم مر الحياة وحلوها دتم لي ضمان الروح وبلسم

الجروح

الى رفيقات دربي وصديقات عمري من قاسمتا عبء البدايات وحلو النهايات
اصبحتم قطعة من روحي

وختاما نسال الله ان يتقبل منا سعينا ويبارك لنا فيه ونحمده حمدا جليلا ونصلي
ونسلم على شفيع الامة تسليما

زينب

Thanks

I, the student Zeyneb, am pleased to express my sincere thanks and appreciation to Dr. Mohammed Yousri Silaa for his continuous support and efforts throughout his supervision of my thesis.

I am grateful to have you as my supervisor. Thank you for your generosity and great influence on me. You are something that cannot be described in words, and if words describe you, they will not do you justice.

You are a symbol of generosity and sincerity. May you always be a beacon of knowledge and a light that illuminates the paths of goodness.

Thank you doctor. May God guide you and reward you with the best of rewards.

الملخص:

تقدم هذه المذكرة نهجًا لإدارة الطاقة بشكل أفضل في أنظمة الطاقة المتجددة، وتحديدًا دمج خلية الوقود مع محولات DC-DC من النوع المعزز الذي يتم التحكم فيه باستخدام تقنيات التحكم في الخطوة الخلفية. تُعد خلايا الوقود، وخاصة خلايا وقود غشاء التبادل البروتوني (PEMFCs) مصدرًا واعدًا للطاقة المتجددة نظرًا لكفاءتها العالية وانبعاثاتها المنخفضة، ولكنها تظهر سلوكًا غير منتظم، مما يشكل تحديات للمراقبة والتحكم. تُعد محولات DC/DC مكونات أساسية لتوصيل مصادر الطاقة المتجددة بالشبكة أو الأحمال الأخرى، مما يوفر تحويلًا فعالاً للطاقة.

يعد التحكم في الخطوة الخلفية (BSC) طريقة تصميم تكرارية تُستخدم لحل ديناميكيات PEMFC غير الخطية وتحسين إدارة طاقة النظام. من خلال دمج BCS مع محولات DC/DC، يهدف النهج المقترح إلى تحسين استقرار النظام، وتحسين كفاءة تحويل الطاقة، وتعظيم استخدام مصادر الطاقة المتجددة. تظهر نتائج المحاكاة فعالية النهج المقترح في ظل الاضطرابات، في تحقيق الإدارة المثلى للطاقة في أنظمة الطاقة الديناميكية مما يدل على إمكاناته لتطبيقات العالم الحقيقي في إنتاج واستهلاك الطاقة المستدامة.

Abstract

This memory presents an approach for better energy management in renewable energy systems, specifically integrating a fuel cell with DC-DC converters type boost controlled with back stepping control techniques. Fuel cells especially proton exchange membrane fuel cell's (PEMFCs) are a promising source of renewable energy due to their high efficiency and low emissions, but they exhibit irregular behavior, which poses challenges for monitoring and control. The DC/DC converters are essential components for connecting for renewable energy sources to the grid or other loads, providing efficient energy conversion.

The back stepping control (BSC), is an iterative design method, which is used to solve the PEMFC nonlinearity dynamics and improve system energy management. By integrating the BCS with DC/DC converters, the proposed approach aims to improve system stability, improve energy conversion efficiency, and maximize the use of renewable energy sources. Simulation results demonstrate the effectiveness of the proposed approach under the disturbances, in achieving optimal energy management in dynamic energy systems demonstrating its potential for real-world applications in sustainable energy production and consumption.

Résumé:

Ce mémoire présente une approche pour une meilleure gestion de l'énergie dans les systèmes d'énergies renouvelables, intégrant spécifiquement une pile à combustible avec des convertisseurs DC-DC de type boost contrôlés avec des techniques de contrôle back stepping. Les piles à combustible, en particulier les piles à combustible à membrane échangeuse de protons (PEMFC), sont une source d'énergie renouvelable prometteuse en raison de leur rendement élevé et de leurs faibles émissions, mais elles présentent un comportement irrégulier, ce qui pose des problèmes de surveillance et de contrôle. Les convertisseurs DC/DC sont des composants essentiels pour connecter des sources d'énergie renouvelables au réseau ou à d'autres charges, assurant une conversion d'énergie efficace.

Le contrôle pas à pas en arrière (BSC) est une méthode de conception itérative utilisée pour résoudre la dynamique de non-linéarité PEMFC et améliorer la gestion de l'énergie du système. En intégrant le BCS aux convertisseurs DC/DC, l'approche proposée vise à améliorer la stabilité du système, à améliorer l'efficacité de la conversion d'énergie et à maximiser l'utilisation des sources d'énergie renouvelables. Les résultats de simulation démontrent l'efficacité de l'approche proposée sous les perturbations, pour parvenir à une gestion optimale de l'énergie dans les systèmes énergétiques dynamiques, démontrant son potentiel pour des applications réelles dans la production et la consommation d'énergie durable.

Summary

General introduction.....	14
ChapterI:.....	15
I.1 Introduction.....	16
I.2 History.....	16
I.3 The fuel cell system	18
I.4 Structure and operating principle of a fuel cell	19
I.5 Technical assembly of fuel cell.....	19
I.6 Fuel cell types	21
I.6.1 Proton exchange membrane(PEMFC).....	22
I.7 Modellingof the pemfc system	26
I.11 Stack modeling PEMFC	32
I.7 Results:.....	34
I.10 Conclusion	35
ChapterII:.....	36
DC-DC converter	36
II.1 Introduction.....	37
II.2 History.....	38
II.3 DC-DC converter	38
II.4 Applications of DC-DC converters	39
II.5 Switching consideration of DC-DC converters:.....	39
II.6 Types of DC-DC converter	40
II.7 Study of DC-DC converters.....	40
II.7.1 The boost converter	40
II.7.2 General boost converter configuration	41
II.8 Block diagram.....	45
II.9 States pace average model	45
II.7 Results.....	49
II.11 Conclusion	54
ChapterIII:	55

BSA and PID-ZN (PID control with Ziegler-Nichols tuning)controller..	55
III.1 Introduction.....	56
III.2 Estimating the reference current(<i>I_{ref}</i>)forPEMFC.....	56
III.3 PI controller	57
III.4 PID controller.....	58
III.5 Ziegler-Nichol frequency domain method(ZN-FDM).....	59
III.6 Back stepping.....	60
III.6.1 Implementation of the back stepping algorithm.....	60
III.7 Results.....	64
III.8 Conclusion	69
General conclusion:.....	70
Bibliography	71

Figures list

Figure 1: Schematic representation of William Grove’s 1839 fuel cell [6]	18
Figure 2: Block Diagram of a Fuel cell Power Plant.	18
Figure 3: (a) operating principle of a PEMFC;(b)PEMFCs stack structure [9]..	19
Figure 4: PEM fuel cell components and assembly [10].	20
Figure 5: shows the PEMFC diagram	22
Figure 6: Electrical equivalent circuit of PEM fuel cell dynamical model	26
Figure 7: <i>E_nernst</i> Simulation model.....	27
Figure8: <i>Vact</i> Simulation model.	28
Figure9: <i>Eohms</i> simulation model.	30
Figure10: <i>Econ</i> Simulation model.....	31
Figure11: fuel cell simulation model.....	31
Figure 12: <i>Vstack</i> Simulation model.....	33
Figure 13: Change in current by voltage and current by power by change in hydrogen pressure and change in temperature:(a) P–I curve under different temperatures and constant pressure;(b) V–I curve under different temperatures and constant pressure;(c) P–I curve under different pressureand constant temperature;(d) V–I curve under different pressure and constant temperature[14].	34
Figure 14: DC-DC power converter.....	37
Figure 15: Circuit diagram of Boost Converter	41
Figure 16: Circuit operation Mode 1	42
Figure 17: Circuit operation Mode 2.....	42
Figure 18: Waveforms [15].	43
Figure 19: Block diagram.....	45
Figure 20: Switch ON equivalent Circuit.....	45
Figure 21: Switch OFF equivalent Circuit	48
Figure 22: DC/DC boost converter simulation model	49
Figure 23: DC-DC step up converter	50
Figure 24: Synoptic diagram of the back stepping algorithm.....	64
Figure 25: a proton exchange membrane fuel cell (PEMFC) under BSA and PID-ZN (PID with Ziegler-Nichols tuning) control strategies: Fuel cell current (IFC) versus time.....	64
Figure 26: a proton exchange membrane fuel cell (PEMFC) under BSA and PID-ZN (PID with Ziegler-Nichols tuning) control strategies: Fuel cell voltage (VFC) versus time	65
Figure 27: a proton exchange membrane fuel cell (PEMFC) under BSA and PID-ZN (PID with Ziegler-Nichols tuning) control strategies: Fuel Cell (PFC) Power vs. Time	66

Figure 28: the performance of a DC-DC boost converter using two different control methods: BSA and PID-ZN (PID control with Ziegler-Nichols tuning): Input Current (I_{Boost}) vs. Time (Seconds) 67

Figure 29: the performance of a DC-DC boost converter using two different control methods: BSA and PID-ZN (PID control with Ziegler-Nichols tuning): Boost voltage (V_{Boost}) versus time (sec)..... 67

Figure 30: the performance of a DC-DC boost converter using two different control methods: BSA and PID-ZN (PID control with Ziegler-Nichols tuning): Output Power (P_{Boost}) vs. Time (Seconds) 68

TABLES LIST

Table 1: Characteriistics of fuel cell types[12].....	21
Table 2: PEM fuel cell parameters	32
Table 3: DC/DC Boost parameters	49
Table 4: Ziegler-Nichol PID tuning parameters	59

List of Abbreviations and Symbols

<i>FC</i>	Fuel cell
<i>PEMFC</i>	Proton-exchange membrane fuel cells
<i>MEA</i>	Membrane electrode assembly
<i>CL</i>	Catalyst layer
<i>ORR</i>	Oxygen reduction reaction
<i>E_{nernst}</i>	Nernst Voltage
<i>T_{FC}</i>	Cell temperature
<i>P_{H2}</i>	Hydrogen gas pressures
<i>P_{O2}</i>	Inlet oxygen
<i>V_{act}</i>	Activation Polarization
<i>I_{FC}</i>	Operating current
ζ_i	Parametric coefficients
<i>CO₂</i>	Oxygen Concentration
<i>R_C</i>	Electron transfer resistance a cross the collector plates
<i>R_M</i>	Proton movement resistance across the solid membrane
ρ_M	Specific resistivity of the membrane
<i>A</i>	The active area of the cell
<i>l</i>	The thickness of the membrane
<i>E_{ohm}</i>	Ohmic Polarization
<i>E_{con}</i>	Concentration Polarization
Ψ	Parametric coefficient that depends on the cell
<i>j</i>	Current density
<i>j_{max}</i>	Maximum current density
<i>P_{FC}</i>	Gross electrical power of the stack
<i>SMPS</i>	Switched-mode power supply
<i>BJT</i>	Power bipolar junction transistor
<i>MOSFET</i>	Power Metal Oxide Semi conductor Field Effect Transistor
<i>GTO</i>	Gate Turn off Thruster
<i>IGBT</i>	Insulated gate bipolar transistor
<i>I_{ref}</i>	Estimating the Reference Current
<i>MPP</i>	Maximum power point
<i>PI</i>	Proportional integral

<i>PID</i>	Proportional integral and derivative
<i>ZN– FDM</i>	Ziegler-Nichol Frequency Domain Method
<i>MZN</i>	Modified Ziegler-Nichol
<i>DOM</i>	Damped Oscillation Method
<i>TLM</i>	Tyreus-Luyben Tuning Method
<i>GGM</i>	Good Gain Method
ε_i	Current Error
<i>BSA</i>	Back stepping

General introduction

In the 21st century, unprecedented energy challenges, such as reducing emissions, diversifying energy sources, and meeting the growing demand, highlight the importance of sustainable energy production systems. Solar photovoltaic (PV) and hydrogen, as cutting-edge technologies, are key pillars in the transition to a cleaner and more sustainable energy future. Many studies have investigated challenges and promising solutions in solar PV green energy and hydrogen production, highlighting the intermittent nature of PV power and the need for energy storage systems to minimize fluctuations. Some studies have identified current gaps and provide recommendations for more accurate and informative modelling to help analysts and policymakers improve the integration of renewable energy. The aim is to ensure continuous and reliable hydrogen production. Many studies have focused on the modelling and simulation of such complex systems. This study aims to model and simulate a Proton Exchange Membrane (PEM) electrolyze cell to better understand the factors affecting the production of hydrogen and oxygen. The difficulties include a precise model, temperature effects [1]. The output voltage of the FCs is not linear. Hence, DC–DC converters are needed to adjust the appropriate input and output voltage levels in order to avoid damage to the FCs and the load. The converter design used for PEMFC has an important role in the efficiency of the total system. For a conventional DC–DC boost converter, duty factor must be kept high in order to obtain high output voltage [2]. The fuel cell transforms hydrogen into DC power. In most stationary and mobile applications, fuel cells are used in conjunction with other power conditioning converters and a circuit model would be beneficial, especially for power electronics engineers who in many cases have the task of designing converters associated with the fuel cell for various load applications [3]. Control of fuel cells using back stepping algorithm to keep the system functioning at its optimal power point. The main feature of this method is its simplicity, robustness, and high tracking performance, confirmed by the obtained results. The fuel cell, the DC–DC converter, and the controllers are presented, modelled, identified, and then tested under a Matlab–Simulink environment. The obtained simulation results are analysed and discussed. Finally, some conclusions are made and future works are suggested [4].

Chapter I:

Fuel cell system

I.1 Introduction

Thanks to technological advancements, the use of different types of fuel has increased ten times. Therefore, people use fossil fuels (oil, gas and coal) to meet their needs daily energy requirement. This has led to the depletion of these resources. While new deposits have been discovered and the use of fossil fuels is another major problem. Burning fossil fuels produces carbon dioxide CO_2 which is released causes a greenhouse effect, CO_2 emissions increased by 1.5% in 2018. Strict the effect leads to an increase in the earth's temperature and thus global warming. Global warming is a serious problem that is causing the polar ice caps to melt. Continued sea level rise may lead to tsunamis and flooding in coastal areas. For this reason pollution, the need for clean and significant energy is necessary the demand for electricity and energy is increasing worldwide due to population growth .To minimize the damage to our environment, the world has done the following in the transition to alternative energy sources began. Renewable energy sources are the cleanest and most environmentally friendly energy source. Great progress has been made in the last decade were built using renewable energy technologies such as solar, wind, tidal, etc. The disadvantage of renewable energy is that it is dependent on external factors such as: sunlight, wind speed, etc. These external factors are uncontrollable and depend entirely on nature. An alternative source of clean energy is use of fuel cells. Fuel cells are the perfect solution to generate eternal energy requirement. Thanks to their properties, they can also be used as a fuel source for unmanned vehicles .The is compact and easy to fuel. Similar study on the lead-acid comparison, and fuel cells for use in unmanned vehicles were developed in .Fuel cells can't do that depends on atmospheric conditions and does not produce pollutants or harmful gases. Scientists are working on reducing production costs so that they can be marketed at an affordable price. [5]

I.2 History

The technology of fuel cells has done a long way since it first was discovered by a Welsh physicist William Grove in 1838 . The first sketch of fuel cells prototype is shown in Figure II.1. Nearly at the same time the work regarding fuel cells was published in Philosophical Magazine by a German-Swiss chemist Christian Friedrich Schoenbein The quick fact list in chronological sequence, provided below shows the development of the fuel cell technology throughout the years:

- 1801: Humphry Davy discovers the principles of electrochemistry
- 1838 : W. Grove invented the gas battery - the first prototype of fuel cell . In the same year, C. F. Schoenbein published work of first electricity generated from hydrogen and oxygen, produced from water.
- 1889: Ludwig Mond and Carl Langer continued the idea and officially used the term fuel cell.
- 1893 : Friedrich Wilhelm Ostwald - one of the founders of physical chemistry, - explained the role of each fuel cells element.
- 1955 – 1958: *The* First prototype of Proton Exchange Membrane (PEM) Fuel Cell was constructed by General Electric. This patent was called Grubb Niedrach fuel cell.
- 1959: Francis Thomas Bacon developed first documented and working stationary fuel cell with rated capacity 5 kW
- 1964: One-man underwater research vessel, that was powered by a 750 – watt fuel cell, again the product of Allis Chalmers company
- 1965: NASA,,s Project Gemini used the fuel cells to produce energy and drinkable water. It is considered as the first commercial use of this technology
- 1990: Solar-Wasserstoff-Bayern, which is the world,,s first solar-powered hydrogen production facility began its work
- 2002: The first rail way transport running on a hydrogen, so-called hydrail, was shown in Val-d'Or, Canada .In the same year, Type 214 submarine, using Siemens Proton Exchange Membrane fuel cell, was built
- 2004 : The first German Autonomous Underwater Vehicle, called DeepC and using the fuel cell to power itself, was shown
- 2008: Honda starts giving to a leasing its first Fuel Cell Electric Vehicle (*FCEV*) – *Honda FCX – V4*. It is the first step in commercialisation of hydrogen fueled automobiles
- 2013: Falkenhagen power to gas station - the first commercial one of its kind, starts the production of hydrogen from the power from grid
- 2016: Toyota Mirai as the first generally affordable hydrogen automobile is on the sale
- 2017: The Hydrogen Council Initiative, the platform for development and encouragement of investments in the hydrogen and fuel cells sphere, starts to function [6].

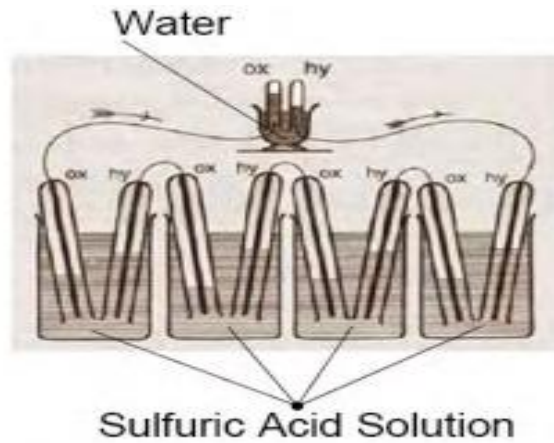


Figure 1: Schematic representation of William Grove's 1839 fuel cell [6]

I.3 The fuel cell system

A fuel cell consists of a series of so-called cells MEA (membrane electrode unit) consisting of: membrane (electrolyte) embedded between two porous membranes electrodes. The battery voltage is indicated by a number cells and the current is determined based on the active surface of the cells. Other parts of the fuel cell system are: pumps and fans, compressors, cooling system, air conditioning (voltage Set the controller so that the DC output of the cell is suitable for the connection electrical

load) and sometimes a DC/AC inverter. Fuel if the fuel cell does not use clean fuel, a conversion system is required hydrogen. A controller is required to coordinate the different parts system. The fuel cell system essentially consists of four sections, as shown in figure 2. To use this system, a mathematical model, system analysis requires software that simulates this Behavior under various working conditions [7].

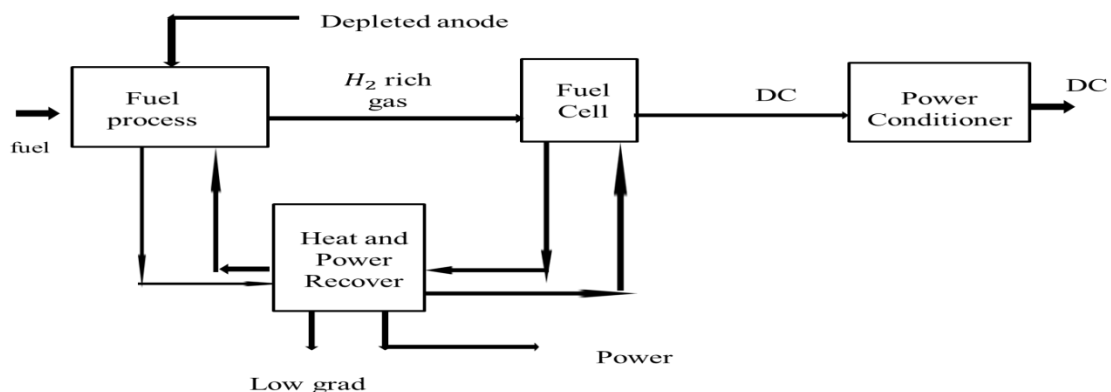


Figure 2: Block Diagram of a Fuel cell Power Plant.

I.4 Structure and operating principle of a fuel cell

A fuel cell consists of two electrodes and an electrolyte layer; the electrolyte is introduced between two electrodes, one anode and the other cathode. Fuel is delivered to the anode, where the fuel oxidation reaction takes place. At the same time an oxidant is supplied to the cathode and a reaction to reduce the oxidant takes place. Occurs when the wires of the two electrodes are connected to an external load form a charging circuit, the charged particles move in the electrolyte and current can flow downloaded from mobile phone .This operating principle of a fuel cell is essentially identical to this one for dry cell and other primary (non-rechargeable) batteries that we all use used daily. However, the reagents are stored in a dry cell, and its shelf life is reached when these reagents are used up. In a fuel cell, see however, the reactants are supplied from outside, so that energy can in principle be generated .Continuously as long as there is a supply of reagents [8].

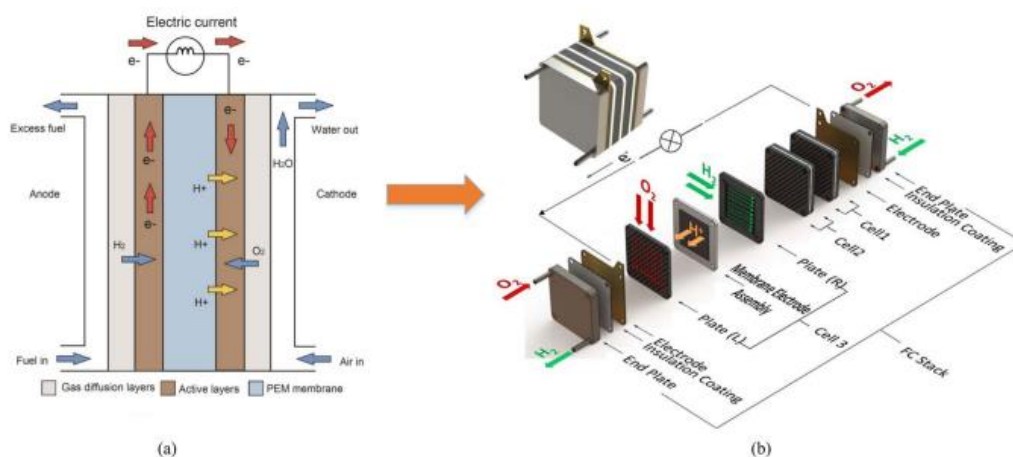


Figure 3:(a) operating principle of a PEMFC;(b)PEMFCs stack structure [9].

I.5 Technical assembly of fuel cell

Fuel cells are static devices meaning the actual cells possess no moving parts and therefore do not need extensive maintenance. However, cooling and control systems guaranteeing optimal working conditions might have moving parts like pumps or fans. Unlike in batteries, the components in fuel cells only act as a catalyst and are not consumed during the reaction – at least under optimal conditions. This means the fuel cell operates as long as it is provided with fuel and does not have to be recharged. This is a major advantage in the transport sector where refueling times can be considered critical. Since the power of one fuel cell is usually not enough to power a car, for example, commercial fuel cell implementations involve multiple

cells in parallel. This can be achieved through space efficient stacking. The Figure 4 shows the schematic of a setup that would be used in a laboratory, for example, and is intended to convey the basic principle. Fuel cell stacks, on the contrary, employ the same components but they are assembled in a much more different way as displayed

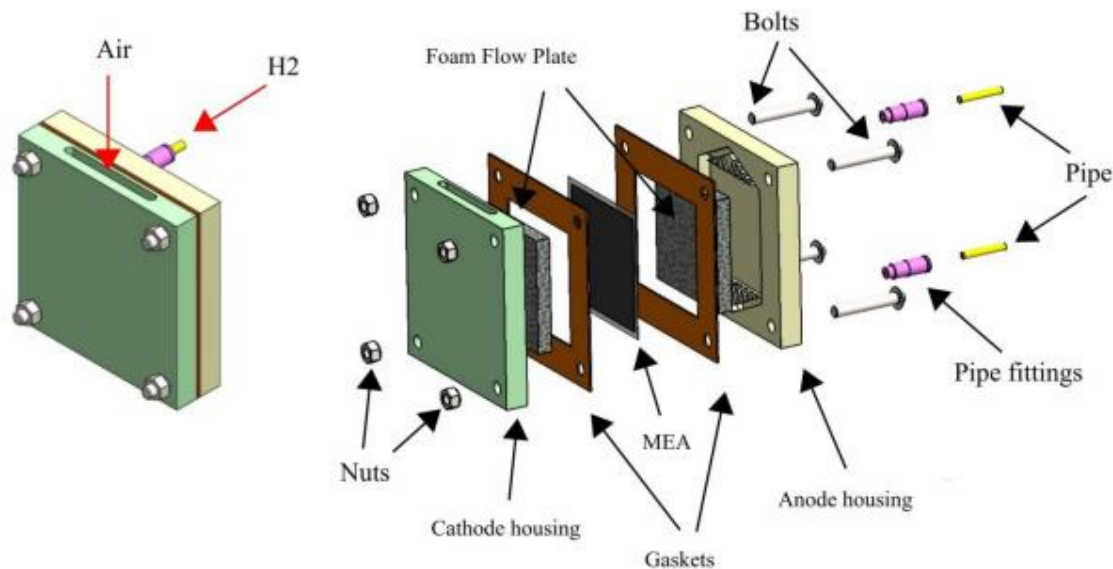


Figure 4: PEM fuel cell components and assembly [10].

The main part of the fuel stack is the membrane electrode assembly (MEA). It consists of cathode and anode electrodes as well as catalyst layers, an ion-conducting electrolyte, and a gas diffusion layer (GDL). The MEA is located by bipolar plates (BPPs). These plates are often made of graphite composite materials and act as current collectors as well as reactant flow controllers. The panels are essential to the fuel cell assembly because they contain a variety of basic functions. They conduct current away from the cell, help with fuel distribution and water management (if necessary), separate individual cells, and facilitate heat regulation. Along with the dipole plate, the coolant gasket helps manage temperature in the same way but also acts as a frame and seal. Gaskets and end plates completely seal the stack and connect it to the fuel as well as the oxidation source [11].

I.6 Fuel cell types

Whereas the 19th Century was the century of the steam engine and, the 20th Century was the century of the internal combustion engine; it is likely that the 21st Century will be the century of the fuel cell systems and hydrogen economy. Fuel cells are now on the verge of being introduced commercially, revolutionizing the way we presently produce power. Fuel cells can use hydrogen as a fuel, offering the prospect of supplying the world with clean, sustainable electrical power.

The integrated energy system of the future would combine large and small fuel cells for domestic and decentralized heat and electricity power generation with local (or more extended) hydrogen supply networks that would also be used to fuel conventional (internal combustion) or fuel-cell vehicles. There are several different types of fuel cells, most often categorized by the type of electrolyte present. Four of the more common fuel cells are proton exchange membrane fuel cells (PEMFC), phosphoric acid fuel cells (PAFC), molten carbonate fuel cells (MCFC), and solid oxide fuel cells (SOFC) [12].

Table 1: Characteristics of fuel cell types[12].

	PEMFC	PAFC	MCFC	SOFC
Electrolyte	Membrane Polymer	Phosphoric Acid	Molten Mixture	Ceramic
Catalyst	Platinum	Platinum	Nickel	Perovskites
Temperature Operation	50 – 80° C	150 – 200° C	≈ 650° C	800 – 1000° C
Output Power Range	50 – 250KW	< 200 KW	10KW – 2MW	< 100KW
Efficiency	40 – 50%	40 – 80%	60 – 80%	~60%
Electrolyte	Membrane Polymer	Phosphoric Acid	Molten Mixture	Ceramic

I.6.1 Proton exchange membrane(PEMFC)

The most popular are the proton exchange membrane fuel cells (PEM). A common type of fuel cell for light transportation applications, because they change their output quickly (e.g. at start up) and do not work well in small applications. The main advantages of PEM are, which respond quickly to changes in power demand, do not leak, do not corrode, and use inexpensive manufacturing materials (plastic membrane) Currently PEMFC and power plants these based on it were developed in many countries, including: China, USA, France, Germany, South Korea and Great Britain. Most of the power plants were delivered in 2006(around 60%) involved powering portable devices. The second largest use (approx.26%) is small stationary power plants. for uninterruptible power supply. Approximately 75% of the work on PEMFC is conducted in industrial organizations, while the remaining 25% is conducted in academic and government organizations figure 5

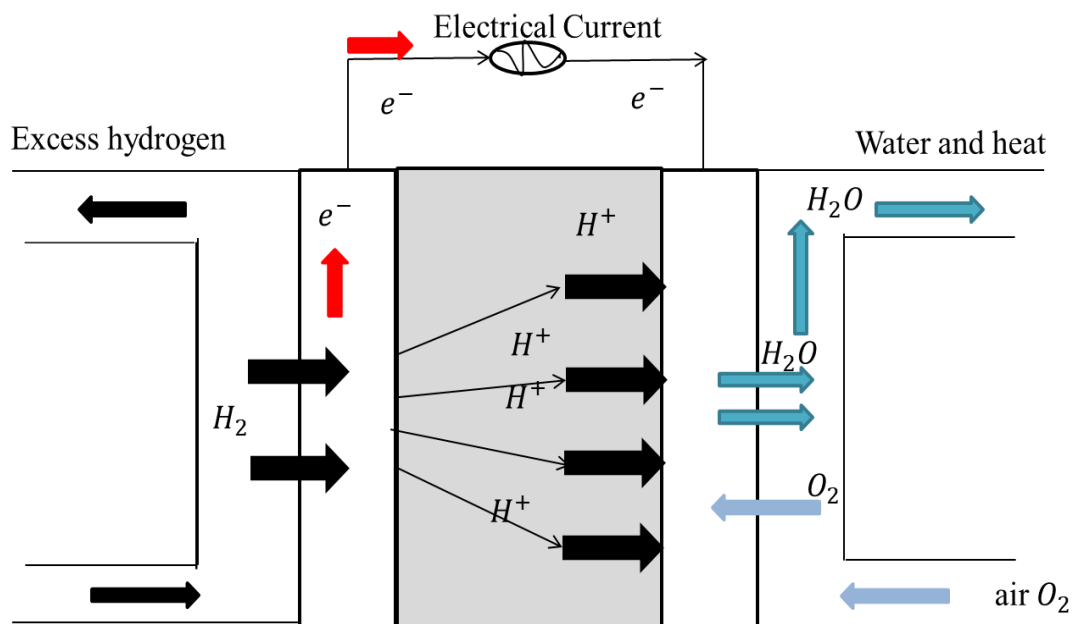


Figure 5:shows the PEMFC diagram

1.6.1.1 Construction materials, operation and efficiency of cells

The proton exchange membrane fuel cells (*PEM*) are made of a solid polymer membrane as an electrolyte consisting of a solid polymer, which consists of an acidified form of to on. The electrolyte conducts hydrogen ions (H^+) from the anode to the cathode. Due Depending on membrane limitations, PEMs operate at temperatures as low as 60 to 100 °C (140 to 212 °F). To achieve sufficient ionic conductivity; the proton-conducting polymer electrolyte requires liquid water. Therefore, Temperatures are limited to less than 100°C, but new developments have made it possible to produce PEM at higher temperatures, up to 200°C (392°F).

The power range of existing PEMs is between approximately 50 W and 150 . Platinum is used as a catalyst because it is the most chemically active substance for the elimination of hydrogen at low temperatures. Waterfall managing in the membrane is critical for efficient operation .The fuel cell must operate under conditions where the water produced as a by product does not evaporate faster than it is produced because the membrane must be hydrated .It is generally lower due to the operating temperature limitation imposed by the polymer compared to 100°C , but very often between 60 and 80°C, and since then If there are problems with the water balance, an H₂-rich gas with a minimum CO content is used. For other fuels, intensive treatment of the fuel is necessary because the anode is easily poisoned by traces of

CO, forms of Sulfur and halo gens. The gaseous reagents are supplied to the battery at a pressure between 2 and 5 bar. This relatively high pressure is not necessary in the car to prevent the membrane from being deflated, the gas from entering the cells, where it is pre-saturated with water vapour until the resulting pressure particle of the gas in the gas-steam mixture reacts weaker. PEMFCs require a source of pure hydrogen to operate. Because hydrogen is not readily available, it is generally produced by reforming a hydrocarbon fuel such as methanol or natural gas. Reformed fuel often contains other gases, such as carbon monoxide, that are harmful to fuel cell operation. Carbon monoxide levels of 50 ppm or more poison the catalyst and cause

severe deterioration in cell performance. Therefore, fuels containing only carbon (e.g. natural gas, methanol, etc.) are not suitable Propane) require further treatment of the fuel. PEMFCs have an electrical efficiency of almost 50%.What is the temperature the waste heat from fuel cells is too low to be used in fuel reforming, the overall system efficiency was therefore

limited to 42%. Depending on the type of reforming process, PEMFC systems can have the lowest electrical efficiency.

All fuel cell systems [13].

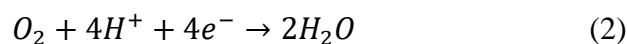
I.6.1.2 Reactions

In a PEM fuel cell two half-cell reactions occur simultaneously, an oxidation reaction at the anode and a reduction reaction at the cathode. These two reactions contribute to the complete reduction of oxidation fuel cell reaction (redox) that produces Water from hydrogen and oxygen gases. Like an electrolyzer the anode and cathode are separated by an electrolyte that allows ions to transfer from one side to the other. The electrolyte of a PEM fuel cell is a solid acid embedded in a membrane. The solid acid electrolyte is saturated with water to allow ion transport.

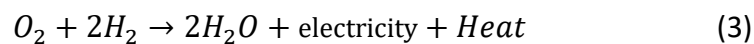
The reactions at the anode are:



The reaction at the cathode is:



His H^+ ion is drawn through the electrolyte from the anode to the cathode by the reactive attraction of hydrogen to oxygen, while electrons are forced through an external circuit. Combining the anode and cathode reactions, the overall cell reaction is:



This exothermic reaction creates water from hydrogen and oxygen gas, has an enthalpy of -286 kilojoules of energy per moles of water were created.

The free energy available to do work decreases with temperature. At a temperature of 25 °C and a pressure of 1 *atmosph*, the energy available for work is approximately -237 *kilojoules* per mole. This energy is observed in the form of electricity and heat[13].

I.6.1.3 Advantages and Disadvantages of using PEM Fuel Cells

The advantages

- Is that they: Use a solid, dry electrolyte. This eliminates liquid handling
- Electrolyte migration and electrolyte replenishment problems. Have low weight and volume with good power-to-weight ratio.
- Operate with quick starts, with full power available in minutes or less.
- Are tolerant of carbon dioxide. As a result, PEM fuel cells can use un- scrubbed air as oxidant, and reformat as fuel.
- Operate at low temperature, so less thermal wear to components.
- Use a non-corrosive electrolyte. Pure water operation minimizes corrosion problems and improves safety.
- Have high voltage, current and power density.
- Operate at low pressure which increases safety.
- Have good tolerance to differential reactant gas pressures.
- Have relatively simple mechanical design.
- Use stable materials of construction.

The disadvantages

Is that they: Operate at low and narrow temperature range which makes thermal management dif cult especially at very high current densities.

- Can tolerate only about 50 ppm carbon monoxide.
- Use an expensive membrane that is dif cult to work with can tolerate only a few ppm of total sulphur compounds
- Need reactant gas humiliation Use an expensive platinum cattily [13].

I.7 Modelling of the pemfc system

In this model, the theoretical thermodynamic potential of the PEM fuel cell is approximately, at a temperature and pressure of 1 atm. However, when we connect the load to the fuel cell, the voltage at the cell terminals decreases compared to the theoretical voltage due to the phenomenon of polarization, due to losses or voltage drops resulting from non-reversibility of the system (also called polarization voltage). . We can distinguish between three forms of polarization: activation polarization, resistance polarization, and concentration polarization, The difference of the activation voltage and the concentration voltage in the fuel cell represented by the resistors (R_{act} and R_{con}), due to the effect of the double charge layer. Knowing that this phenomenon occurs when there is an accumulation of charges between two different materials which are in direct connection, the charge layer in front of the electrolyte electrode behaves like a capacitor. Then we can trace the equivalent electrical circuit of the heat pump as follows:

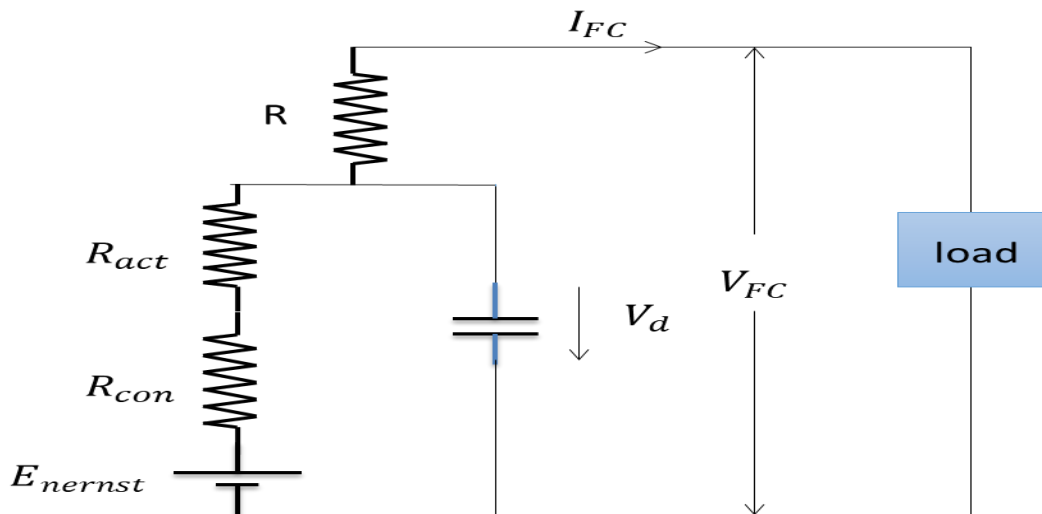


Figure 6: Electrical equivalent circuit of PEM fuel cell dynamical model

So the battery voltage (V_{FC}) is expressed as follows [14]:

$$V_{FC} = (E_{nernst} - V_{act} - V_{ohm} - V_{conc}) \quad (4)$$

- **Nernst Voltage**

The Nernst voltage represents the reversible thermo dynamic voltage of the electrochemical reaction, which is given as follows [14]:

$$E_{nernst} = 1.229 - 0.85 \times 10^{-3}(T_{FC} - 298.15) + 4.31 \times 10^{-5} \times T_{FC} \times \left[\ln(P_{H_2}) + \frac{1}{2} \ln(P_{O_2}) \right] \quad (5)$$

Where T_{FC} is the cell temperature, and P_{O_2} and P_{H_2} are the inlet oxygen and the hydrogen gas pressures, respectively [14].

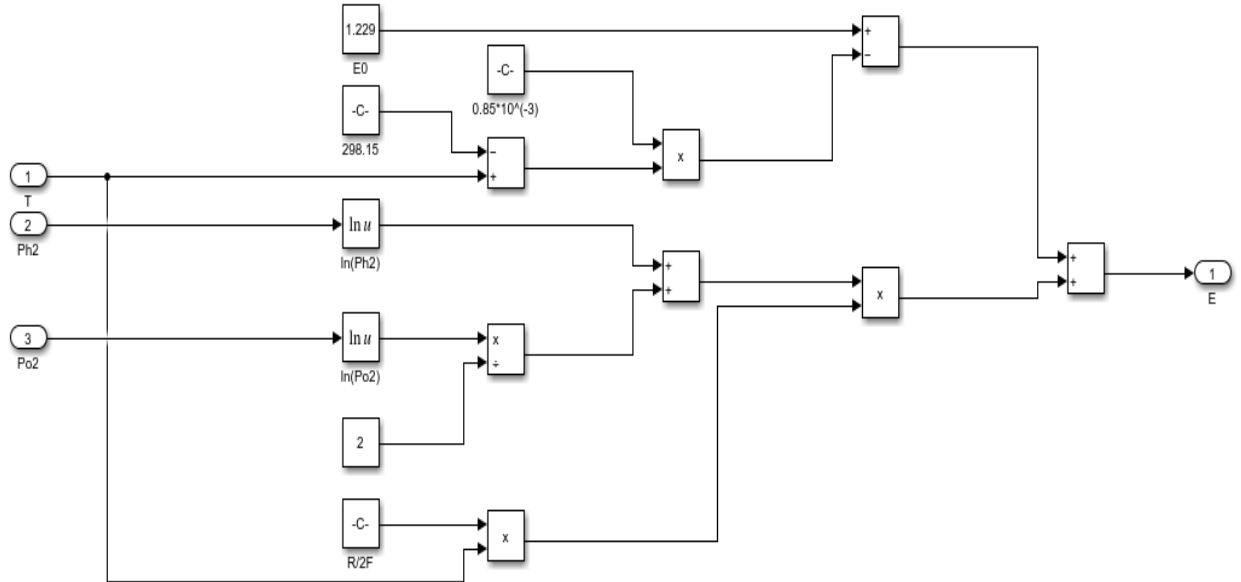


Figure 7: E_{nernst} Simulation model.

- **Activation Polarization**

The activation polarization occurs due to the electrochemical reactions which require a certain amount of energy to overcome the energy barrier for the electrochemical reaction to proceed [14].

$$V_{act} = -[\xi_1 + \xi_2 \cdot T + \xi_3 \cdot T \cdot \ln([CO_2]) + \xi_4 \cdot T \cdot \ln(I_{FC})] \quad (6)$$

Where I_{FC} the operating current and the parameters is $\zeta_{1,2,3,4}$ represent the parameter coefficients for each PEMFC model. The term CO_2 is the oxygen Concentration in the cathode catalytic interface (mol/cm^3) which is given as Follows [14]

$$[CO_2] = \frac{P_{O_2}}{5.08 \times 10^6 \times e^{(-498/T)}} \quad (7)$$

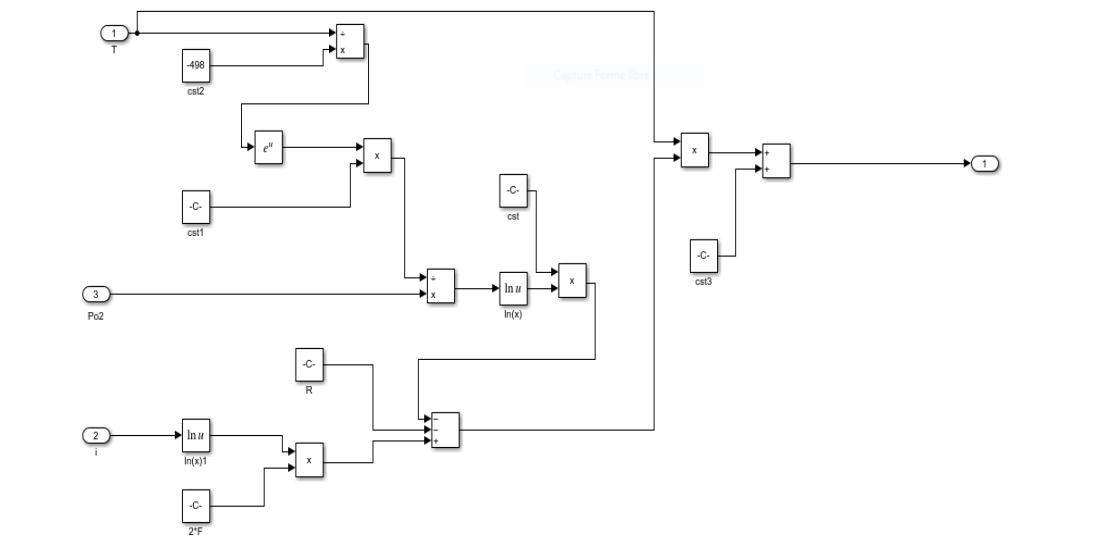


Figure8: V_{act} Simulation model.

- **Ohmic Polarization**

The ohmic polarization results from the electron transfer resistance across the collector plates and carbon electrodes, denoted R_C , and the proton movement resistance across the solid membrane, denoted R_M . The equivalent membrane resistance is given as follows [14]:

$$R_M = \frac{l \times \rho_M}{A} \quad (8)$$

Where ρ_M is the specific resistivity of the membrane (*Ohm.m*), A is the active area of the cell (cm^2), and l is the thickness of the membrane in *cm*.

$$\rho_M = \frac{181,6[1+0,03\left(\frac{I_{FC}}{A}\right)+0,062\left(\frac{T_{FC}}{303}\right)^2\left(\frac{I_{FC}}{A}\right)^{2,5}]}{\left[\gamma-0.634-3\left(\frac{I_{FC}}{A}\right)\right]\exp\left[4.18\left(\frac{T_{FC}-303}{T_{FC}}\right)\right]} \quad (9)$$

Therefore, the ohmic polarization is given as follows [14]:

$$E_{ohm} = I_{FC}(R_M + R_C) \quad (10)$$

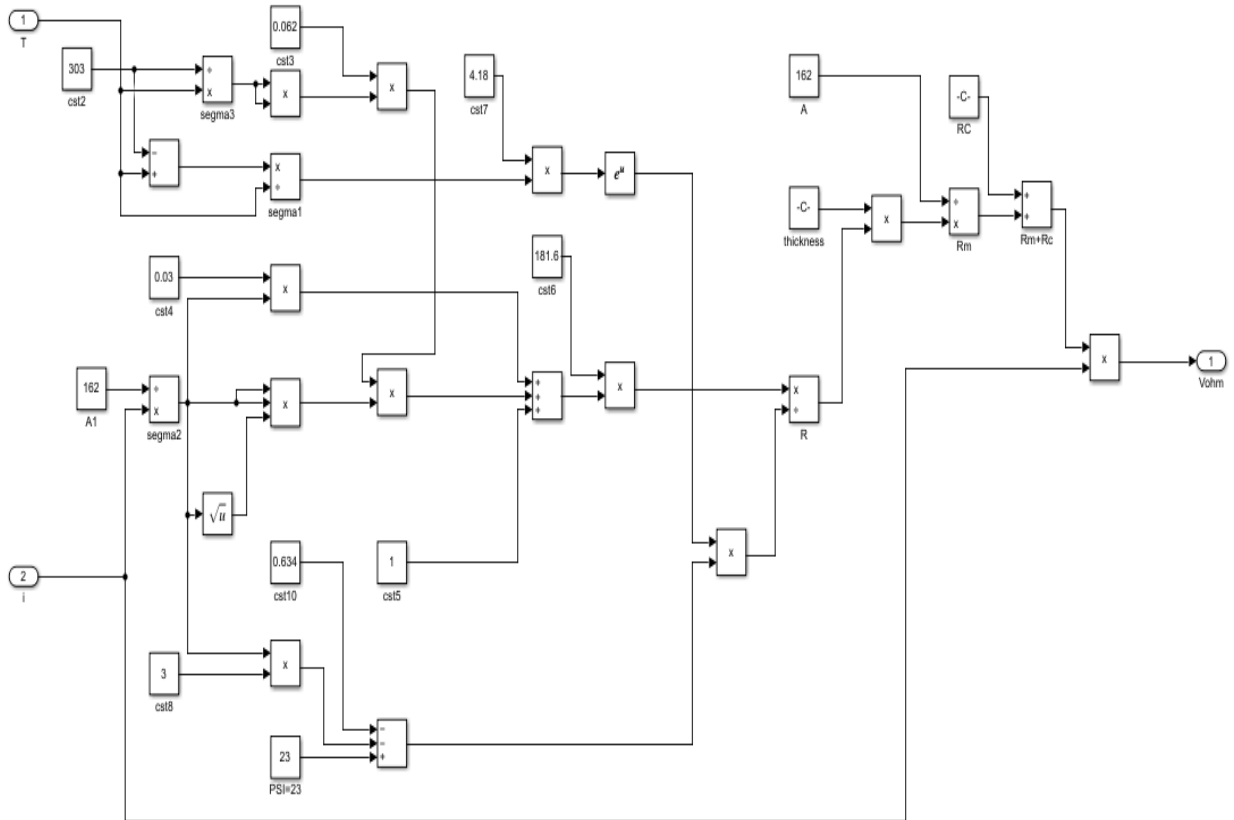


Figure9: E_{ohm} simulation model.

- **Concentration Polarization**

The concentration polarization occurs due to the diminution in the density of the reacting materials. This polarization can be calculated using Equation [14].

$$E_{con} = \psi \cdot \ln\left(1 - \frac{j}{j_{max}}\right) \quad (11)$$

Where ψ is a parametric coefficient that depends on the cell, j represents the cell current density in $.cm^2$, and j_{max} is the maximum current density Overall PEMFC stack output power is given as follows [14]:

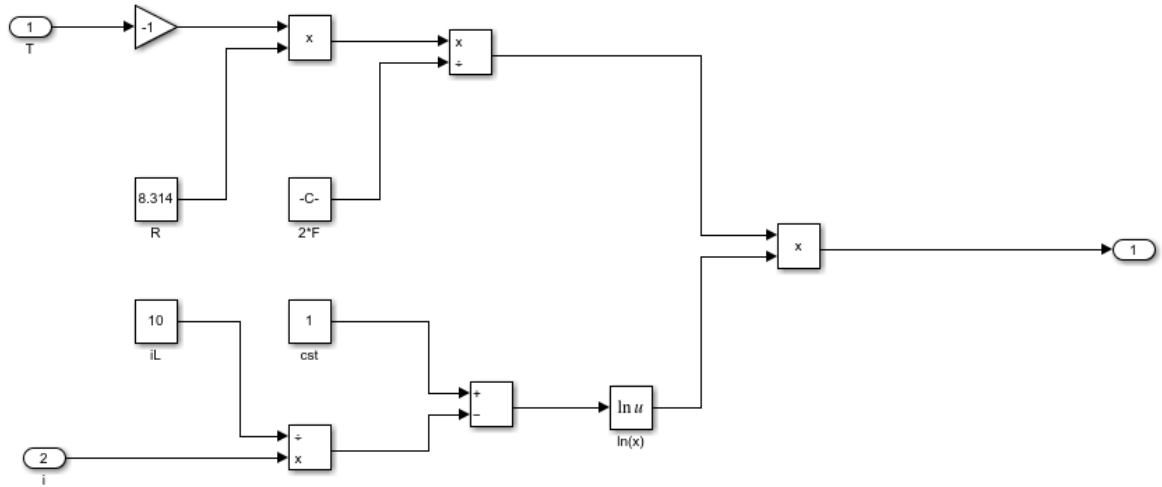


Figure10: E_{con} Simulation model.

$$P_{FC} = V_{FC} * I_{FC} * N_{cells} \quad (12)$$

The final voltage generated by the fuel cell is the sum of the ideal voltage and three losses [12].

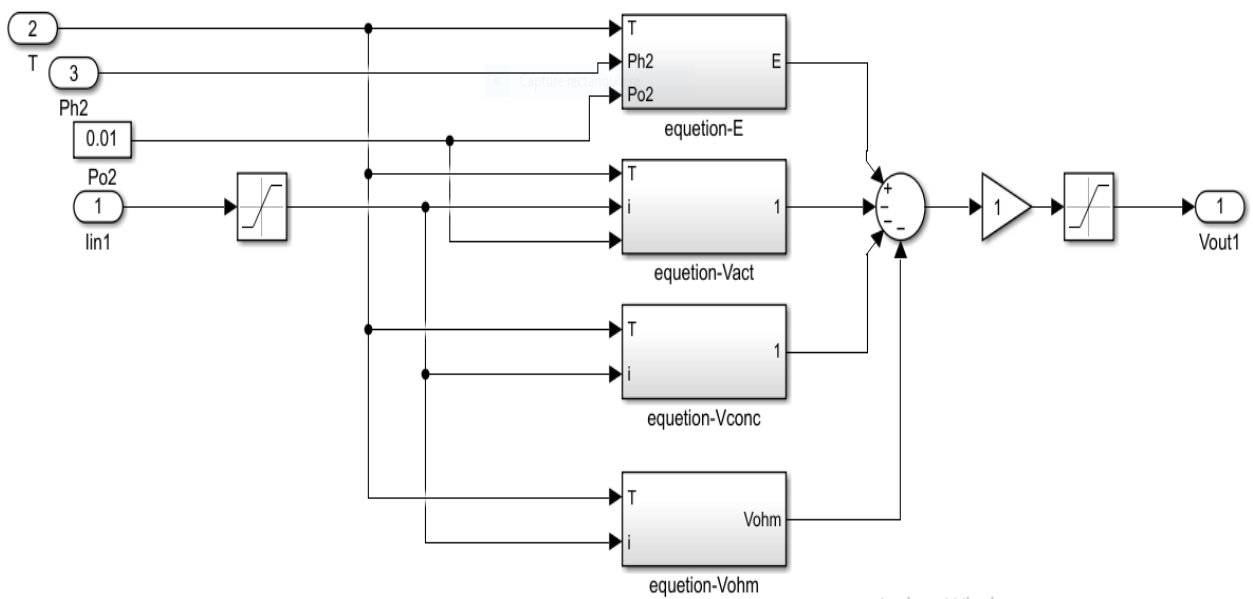


Figure11: fuel cell simulation model

Table 2:PEM fuel cell parameters

Parameters	Value
ξ_1	0.9514 V
ξ_2	$-0.00312 \text{ V}/K$
ξ_3	$-7.4 * 10^{-5} \text{ V}/K$
ξ_4	$1.87 * 10^{-4} \text{ V}/K$
A	162 cm^2
l	$175 * 10^{-6} \text{ cm}$
Γ	23
j_{max}	0.062 A. cm^{-1}
R_C	0.0003
N_{cells}	10
ψ	0.1V

I.11 Stack modeling PEMFC

For both the steady state and dynamic model, the calculated values are for a single cell. A fuel cell consists of a number of cells arranged in such a way that it is called a fuel cell array. The total output voltage can be calculated by taking the product of V_{cell} and the total number of cells

$$V_{stack} = n * V_{cell} \quad (13)$$

The total power output of the fuel cell stack can be calculated by taking the product of current „ i “ and the output voltage V_{stack} [5].

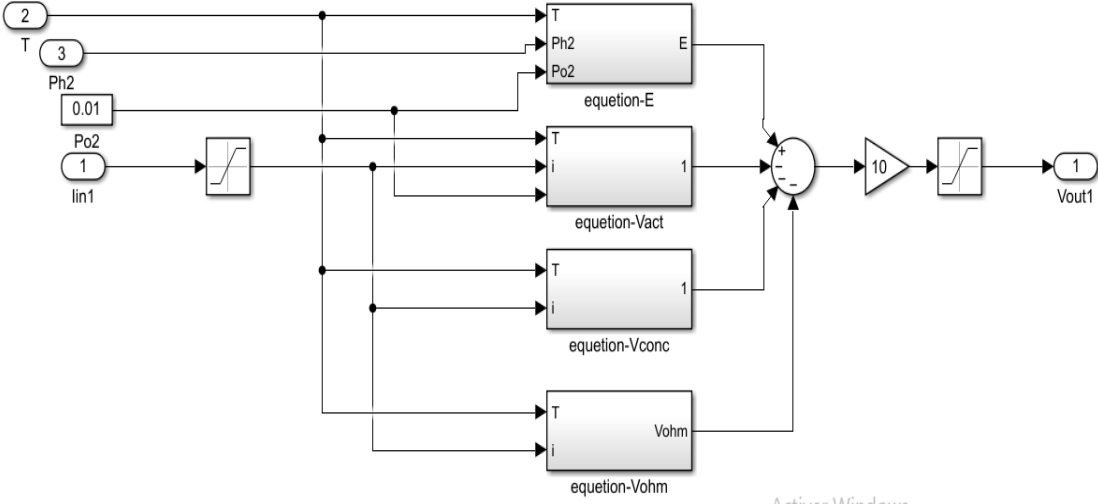


Figure 12: V_{stack} Simulation model

I.7 Results:

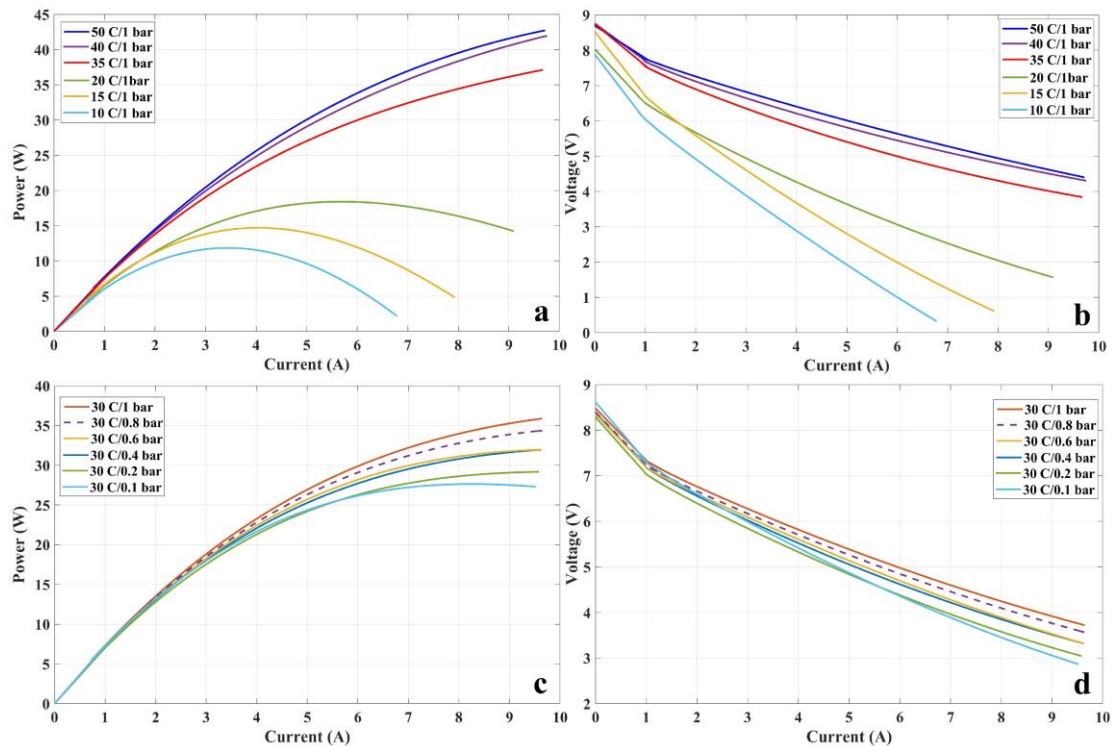


Figure 13: Change in current by voltage and current by power by change in hydrogen pressure and change in temperature: (a) P–I curve under different temperatures and constant pressure; (b) V–I curve under different temperatures and constant pressure; (c) P–I curve under different pressure and constant temperature; (d) V–I curve under different pressure and constant temperature [14].

a) P–I curve under different temperature and constant pressure; shows the effect of temperature on the power of the PEMFC. As the temperature increases, the power of the PEMFC increases.

(b) V–I curve under different temperature and fixed pressure; shows the effect of temperature on the performance of the PEMFC. As the temperature increases, the current increases at a certain voltage.

c) P–I curve under different pressure and fixed temperature; shows effect of pressure on the power of the PEMFC. As the pressure increases, the power of the PEMFC increases.

(d) V–I curve under different pressure and fixed temperature; shows the effect of pressure on the performance of the PEMFC. As the pressure increases, the current density increases at a certain voltage.

Overall, both higher temperatures and increased pressures contribute to improved performance of the PEMFC

I.10 Conclusion

This chapter provides a comprehensive exploration of proton exchange membrane fuel cells (PEMFC), covering their history, architecture, operating principles, assembly, and types. We focus specifically on PEMFCs, a prominent variant in modern applications. In addition, we discuss construction materials, efficiency, and system interactions, and present modeling techniques for PEMFC systems. A mathematical model and an equivalent circuit model of PEMFC are developed and simulated in Matlab–Simulink, with a thorough analysis of the result

ChapterII:

DC-DC converter

II.1 Introduction

In many technical applications, it is required to convert a constant voltage DC source to a variable voltage DC output. The DC-DC conversion converter directly converts the voltage from DC to DC and is simply known as a DC converter. A DC converter is equivalent to an AC converter with a continuously variable turns ratio. It can be used to step down or step up a DC voltage source, as a transformer.

DC converters are widely used to control traction motors in electric cars, trolley cars, marine cranes, forklift trucks, and mine conveyors. They offer high efficiency, good acceleration control and quick dynamic response. They can be used in regenerative braking of DC motors to return power to the supply. This feature saves energy for conveyor systems with frequent stops. DC converters are used in DC voltage regulators; They are also used, with an inductor in conjunction, to generate a DC source, specifically for a current source inverter. [15].

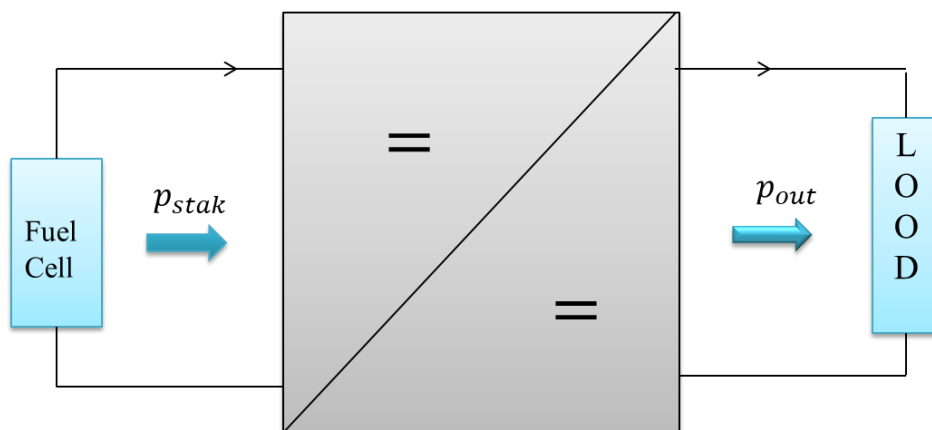


Figure 14:DC-DC power converter

II.2 History

For high efficiency, an SMPS switch must turn on and off quickly and have lower losses.

The advent of commercial semiconductor switches such as the boost converter in the 1950s represented a major milestone that made SMPSs possible. Mains DC to DC converters developed in the early 1960s when semiconductor switches were available. Switched systems such as SMPs are a design challenge because their pattern depends on whether the switch is open or closed. RD Middlebrook of Caltech in 1977 popularized the models of DC to DC converters on today's market. He averaged the circuit configurations for each switching state in a technique called mean space modeling. This simplification resulted in a reduction of two systems to one. This model led to insightful design equations that helped SMPs grow [15].

II.3 DC-DC converter

DC-DC converters are power electronic circuits that convert DC voltage to a different voltage level. There are different types of conversion methods such as electronic, linear, switched mode, magnetic, and capacitive. The circuits described in this report are classified as switched-mode DC-DC converters. These are electronic devices that are used when DC electrical power needs to be changed from one voltage level to another. In general, the use of transformer or switches for the purpose of power conversion can be considered as SMPS. From now on when we mention

DC-DC converters we will address them in relation to SMPS. Some applications where DC-DC converters are important are where the 5V DC on a PC motherboard must be stepped down to 3V, 2V or less for one of the newer CPU chips; Where it needs to be 1.5 volts from a single cell up to 5 volts or more, to operate electronic circuits. In all of these applications, we want to change DC power from one voltage level to another, wasting as little as possible in the process. In other words, we want to

perform the conversion as efficiently as possible. DC-DC converters are needed because unlike AC, DC cannot simply be stepped up or down with a transformer. In many ways, a DC-

DC converter is the DC equivalent of a converter. They basically change the input power to a different impedance level. Whatever the output voltage level, all the output power comes from the input; there is no power generated inside the transformer. Quite the contrary, in fact, some are inevitably used by converter circuits and components, in doing their job [16].

II.4 Applications of DC-DC converters

1. Dc converters can be used in regenerative braking of dc motors to return energy back into the supply and this feature results in energy savings for transportation system with frequent stops. As for example :
 - a) Traction motor control in electric automobiles
 - b) Trolley cars
 - c) Marine Hoists
 - d) Forklift trucks
 - e) Mine Haulers
2. Also used in DC voltage regulators and also are used in conjunction with an inductor to generate a dc current source especially for the current source inverter[16].

II.5 Switching consideration of DC-DC converters:

The converter switch can be implemented by using

- a) Power bipolar junction transistor (BJT)
- b) Power Metal Oxide Semiconductor Field Effect Transistor (MOSFET)
- c) Gate Turn Off Thyristor (GTO)
- d) Insulated gate bipolar transistor (IGBT)

Practical devices have a finite voltage drop ranging from $0.5V$ to $2V$ but during the calculations for the sake of simplicity of the understanding, these switches are considered lossless [16].

II.6 Types of DC-DC converter

There are different kinds of DC-DC converters. A variety of the converter names are included here:

1. The BUCK converter
2. The BOOST converter
3. The BUCK-BOOST converter
4. The CUK converter
5. The Fly-back converter
6. The Forward Converter
7. The Push-pull Converter
8. The Full Bridge converter
9. The Half Bridge Converter
10. Current Fed converter
11. Multiple output converters[16].

II.7 Study of DC-DC converters

There are a variety of possible DC-Dc converters. But from the list of adapters the BOOST adapter will be described

II.7.1 The boost converter

A boost converter (step-up converter) is a power converter with an output DC voltage greater than its input DC voltage. It is a class of switching mode power supply (*SMPS*) containing at least two semi-conductors switches (a diode and a transistor) and at least one energy storage element.

Filters made of capacitors (sometimes in combination with inductors) are normally added to the output of the converter to reduce output voltage ripple. A boost converter is sometimes

called a step-up converter since it “steps up” the source voltage. Since power ($P = VI$) must be conserved, the output current is lower than the source current.

The boost converter has the same components as the buck converter, but this converter produces an output voltage greater than the source.

"Boost" converters start their voltage conversion with a current flowing through the inductor (switch is closed). Then they close the switch leaving the current no other path to go than through a diode (functions as one way valve) The current then wants to slow really fast and the only way it can do this is by increasing it's voltage (akin to pressure) at the end that connects to the diode, and switch. If the voltage is high enough it opens the diode, and one through the diode, the current can't flow back. This is the very basic concept of boost converter [16].

II.7.2 General boost converter configuration

In a boost converter, the output voltage is greater than the input voltage – hence the name “boost”. A boost converter using a power MOSFET is shown below.

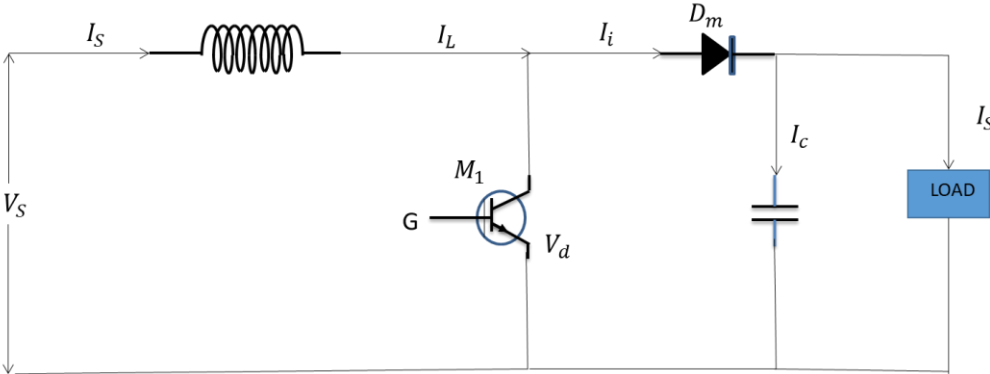


Figure 15: Circuit diagram of Boost Converter

The function of the boost converter can be divided into two modes, mode 1 and mode 2. **Mode 1:** starts when transistor M_1 is turned on at $t = 0$. The input current rises and flows through inductor L and transistor M_1 .

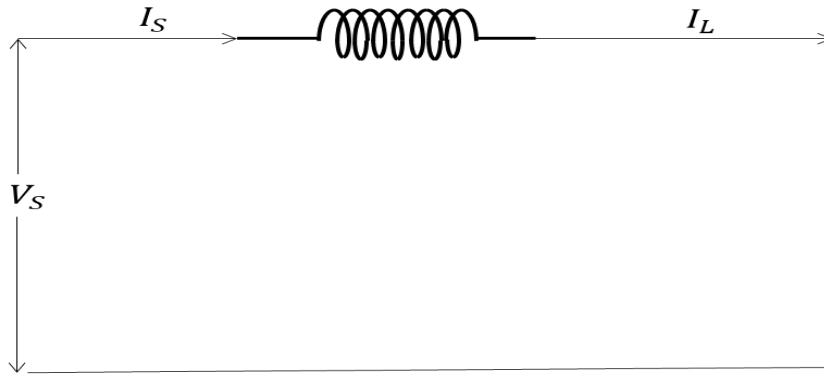


Figure 16: Circuit operation Mode 1

Mode 2: starts when transistor $M1$ is turned off at time $t = t_1$. The input current now flows through L , C , the load and the diode D_m .

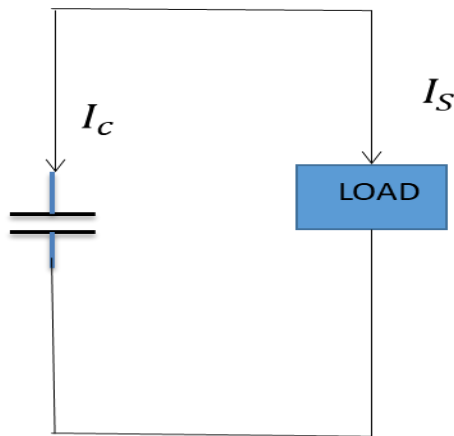


Figure 17: Circuit operation Mode 2

The inductor current decreases until the next cycle. The energy stored in the inductor L flows through the load [15].

The waveforms for the voltages and currents are shown below

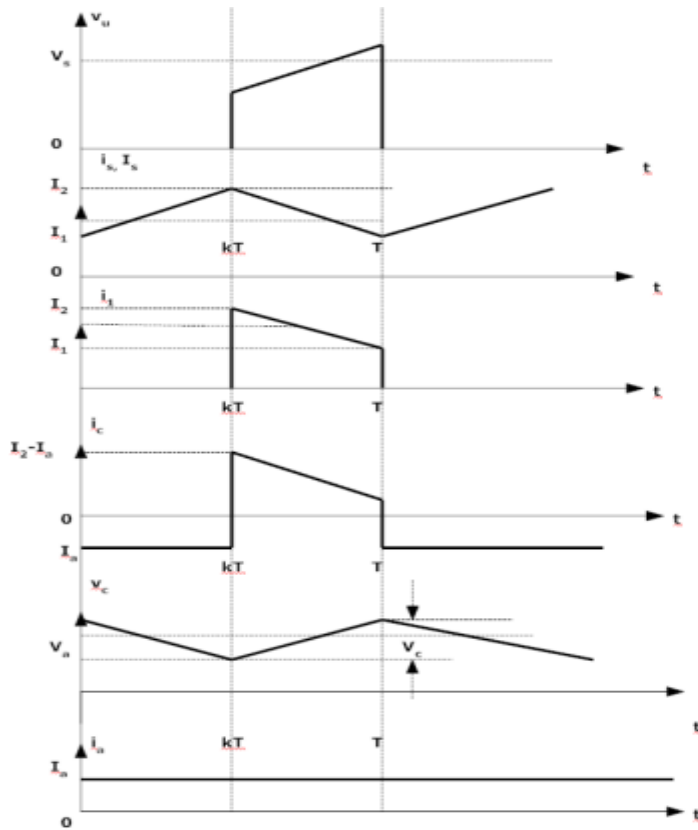


Figure 18: Waveforms [15].

The voltage-current relation for the inductor L is:

$$i = \frac{1}{L} \int_0^T V dt + i_0 \quad (1)$$

OR

$$V = L \frac{di}{dt} \quad (2)$$

For a constant rectangular pulse:

$$i = \frac{Vt}{L} + i_0 \quad (3)$$

When the transistor M_1 is switched:

$$i_{pk} = \frac{(V_{in} - V_{Trans})T_{on}}{L} + i_0 \quad (4)$$

OR

$$\Delta i = \frac{(V_{in} - V_{Trans})T_{on}}{L} \quad (5)$$

And when the transistor is switched off the current is:

$$i_0 = i_{pk} = \frac{(V_{out} - V_{in} + V_D)T_{off}}{L} \quad (6)$$

OR

$$\Delta i = \frac{(V_{out} - V_{in} + V_D)T_{off}}{L} \quad (7)$$

Here V_D is the voltage drop across the diode D_m , and V_{Trans} is the voltage drop across the transistor M_1 .

By equating through Δi , we can solve for V_{out} :

$$\left\{ \begin{array}{l} \frac{(V_{in} - V_{Trans})T_{on}}{L} = \frac{(V_{out} - V_{in} + V_D)T_{off}}{L} \\ V_{in} - V_{Trans}D = (V_{out} + V_D)(1 - D) \\ V_{out} = \frac{V_{in} - V_{Trans}D}{(1 - D)} - V_D \end{array} \right. \quad (8)$$

Neglecting the voltage drops across the diode and the transistor:

$$V_{out} = \frac{V_{in}}{(1 - D)} \quad (9)$$

II.8 Block diagram

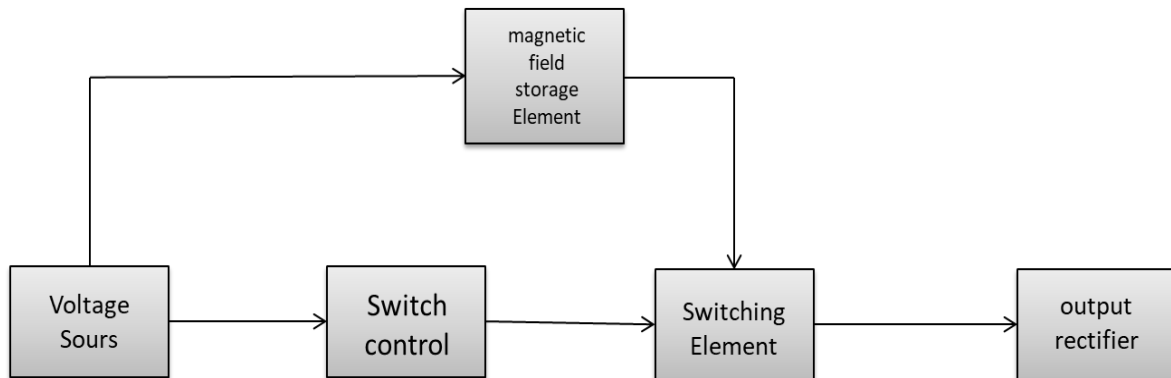


Figure 19:Block diagram

Figure 19 shows the basic blocks of building a boost converter circuit

The circuit receives its DC input voltage from a source. This voltage is used by the switch control unit and also by the element responsible for storing the magnetic field

The module housing the switch controls directs the operation of the switching component

While the rectifier and filter at the output provide a usable DC voltage

II.9 States pace average model

Switch ON equivalent circuit

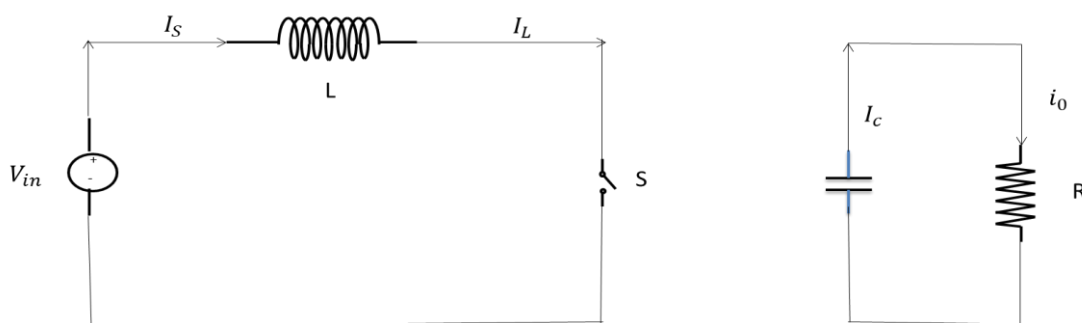


Figure 20: Switch ON equivalent Circuit

$$L \frac{di}{dt} = V_{in} - R_{on} * i_L - R_L * i_L \quad (10)$$

$$V_{out} = i_0 * R \quad (11)$$

$$C \frac{dV_C}{dt} + \frac{V_{out}}{R} = 0 \quad (12)$$

And

$$V_{out} = V_C + i_C * R_C \quad (13)$$

$$V_{out} = V_C \left[\frac{R}{R_C} \right] \quad (14)$$

$$C \frac{dV_C}{dt} = \frac{-V_C}{R+R_C} \quad (15)$$

$$i_{in} = i_L \quad (16)$$

State equation matrices are given as:

$$\begin{bmatrix} di_L/dt \\ dV_C/dt \end{bmatrix} = \begin{bmatrix} (-R_{on} + R_L)/L & 0 \\ 0 & -1/C(R + R_C) \end{bmatrix} \begin{bmatrix} i_L \\ V_C \end{bmatrix} + \begin{bmatrix} 1/L \\ 0 \end{bmatrix} \quad (17)$$

And

$$V_{out} = \begin{bmatrix} 0 & R/(R + R_C) \end{bmatrix} \begin{bmatrix} i_L \\ V_C \end{bmatrix} \quad (18)$$

So, X, W, Y, Z parameters are

$$X_{on} = \begin{bmatrix} (-R_{on} + R_L)/L & 0 \\ 0 & -1/C(R + R_C) \end{bmatrix} \quad (19)$$

$$W_{on} = \begin{bmatrix} 1/L \\ 0 \end{bmatrix} \quad (20)$$

$$Y_{on} = \begin{bmatrix} 0 & R/(R + R_C) \end{bmatrix} \quad (21)$$

$$Z_{on} = [0] \quad (22)$$

$$L \frac{di}{dt} = V_{in} - R_{on} * i_L - R_L * i_L - V_{out} = i_L * R_D \quad (23)$$

$$i_C = i_L - i_R \quad (24)$$

And

$$V_{out} = V_C + i_C * R_C \quad (25)$$

$$V_{out} = V_C \left[\frac{R}{(R + R_C)} \right] + i_L * R_C \left\{ \frac{R}{(R + R_C)} \right\} \quad (26)$$

OR

$$V_{out} = V_C \left[\frac{R}{(R + R_C)} \right] + i_L \left[\frac{R}{(R + R_C)} \right] \quad (27)$$

From above equation

$$L \frac{di_L}{dt} - \left[R_D + R_{on} + R_L + \left(\frac{R * R_D}{R + R_C} \right) \right] i_L - V_C \left[\frac{R}{(R + R_C)} \right] \quad (28)$$

Also

$$i_C = i_L - i_R \quad (29)$$

$$C \frac{dV_C}{dt} = \frac{R}{R + R_C} * i_L - \frac{V_C}{R + R_C} \quad (30)$$

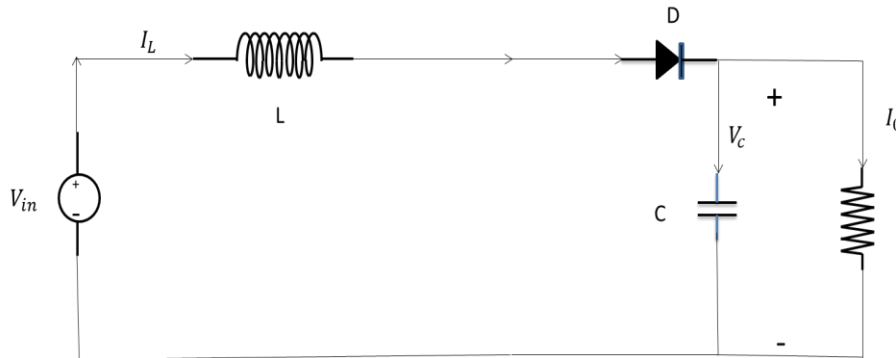


Figure 21: Switch OFF equivalent Circuit

State equation matrices are given as-

$$\begin{bmatrix} di_L/dt \\ dV_C/dt \end{bmatrix} = \begin{bmatrix} -R_{on} + R_L + \frac{R * R_C}{R + R_C} + \frac{R_D}{L} & -\frac{R}{(R + R_C)L} \\ \frac{R}{(R + R_C)C} & -\frac{1}{(R + R_C)V} \end{bmatrix} \begin{bmatrix} i_L \\ V_C \end{bmatrix} + \begin{bmatrix} 1/L \\ 0 \end{bmatrix} V_{in}$$

$$V_{out} = \begin{bmatrix} R * R_C / (R + R_C) & R / (R + R_C) \end{bmatrix} \begin{bmatrix} i_L \\ V_C \end{bmatrix} \quad (32)$$

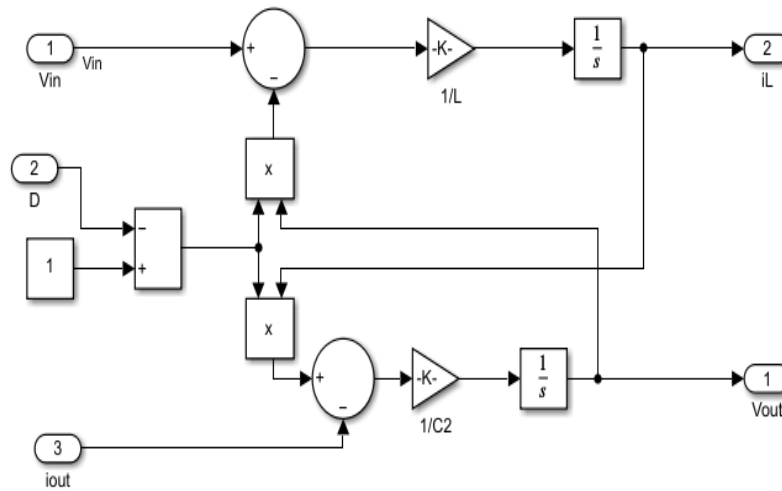


Figure 22: DC/DC boost converter simulation model

Table 3: DC/DC Boost parameters

Parameter	Value
Inductance	69 Mh
Capacitor	1.5 Mf
input voltage	5 V
Resistance load	100Ω

II.7 Results

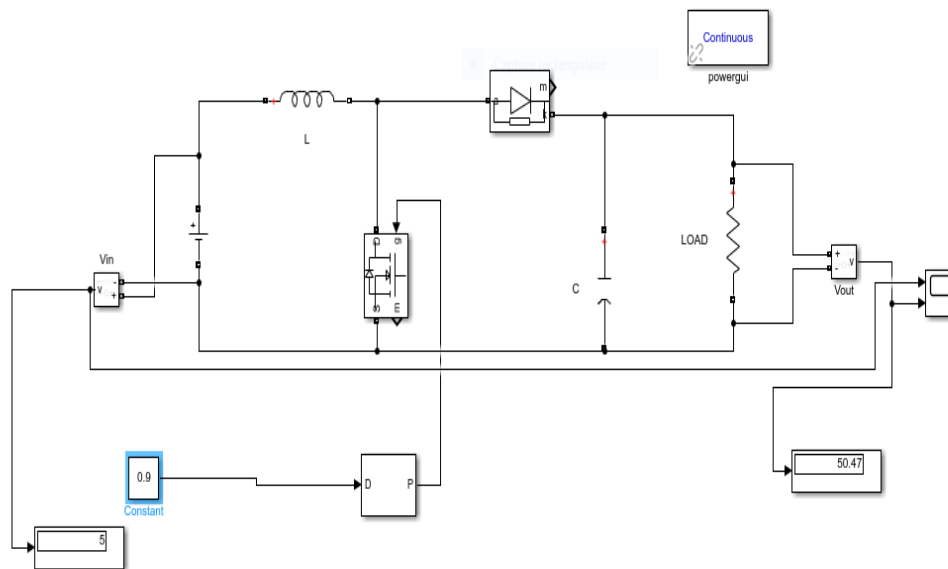
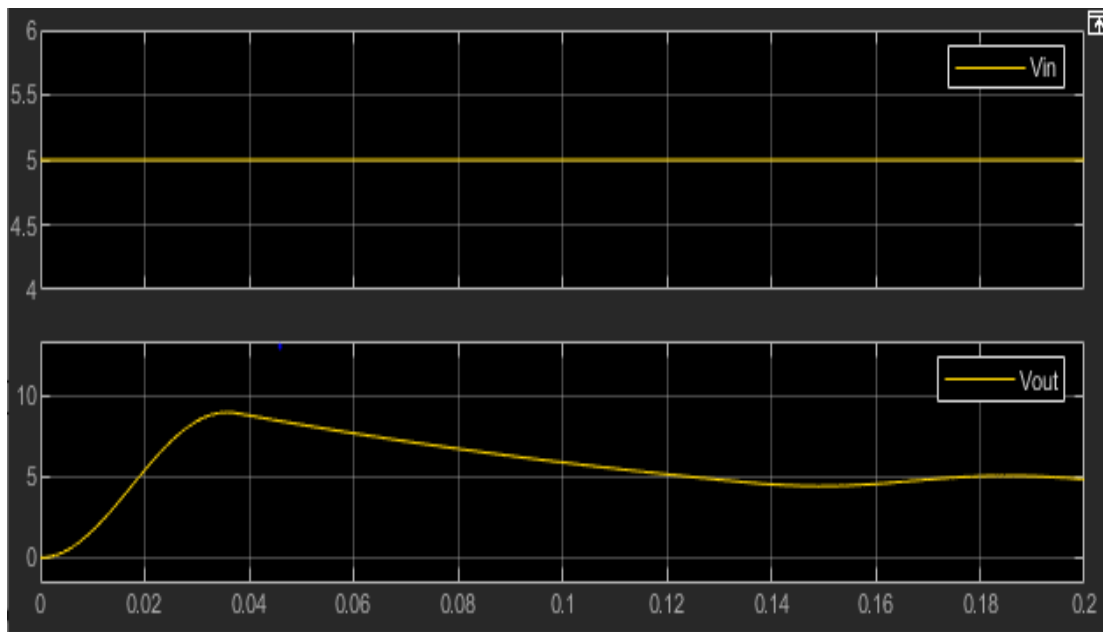
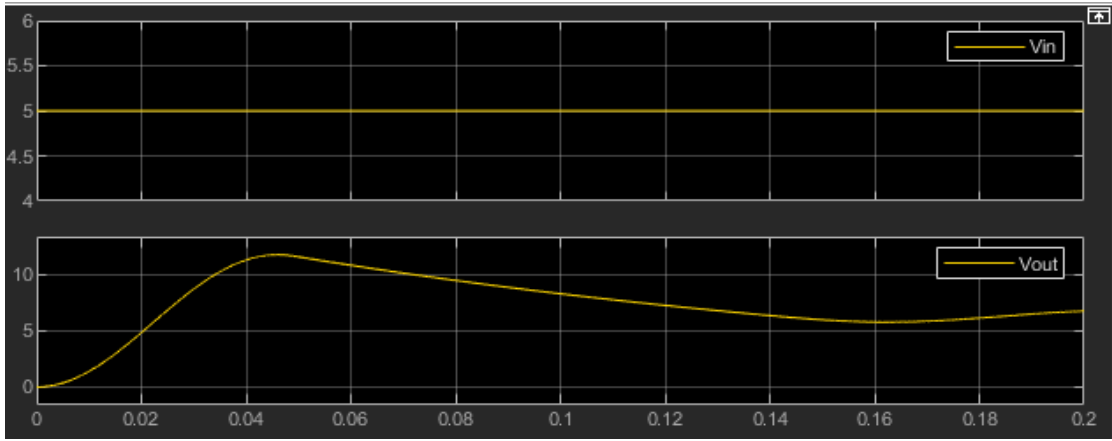


Figure 23: DC-DC step up converter

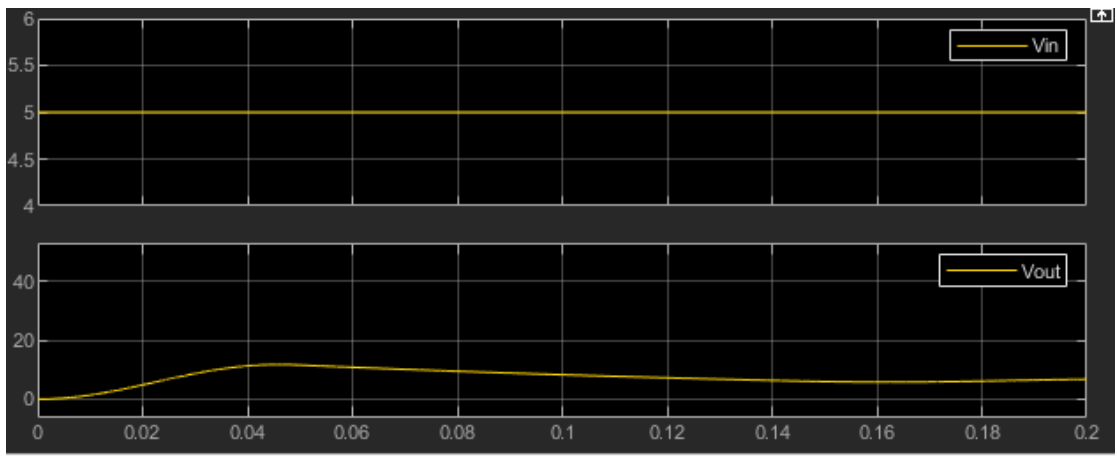
$D=0.1$



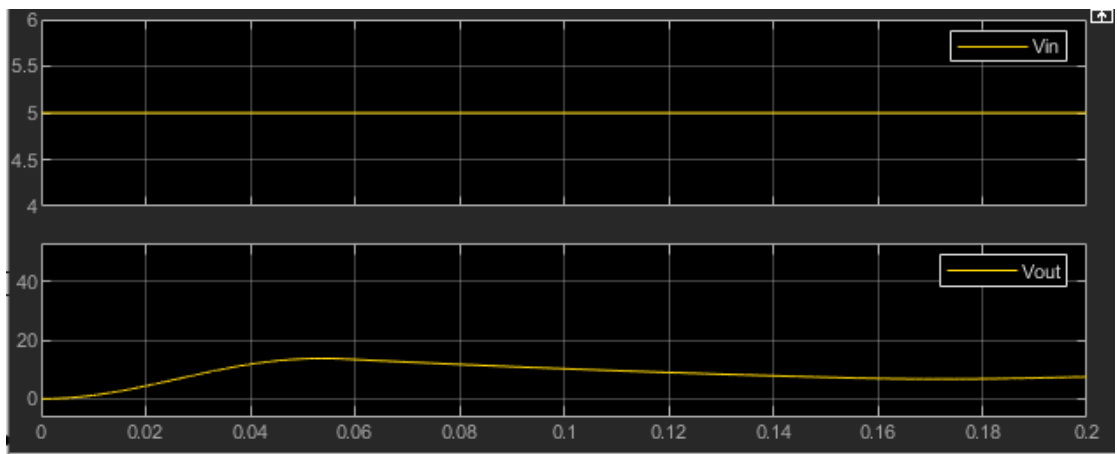
$D=0.2$



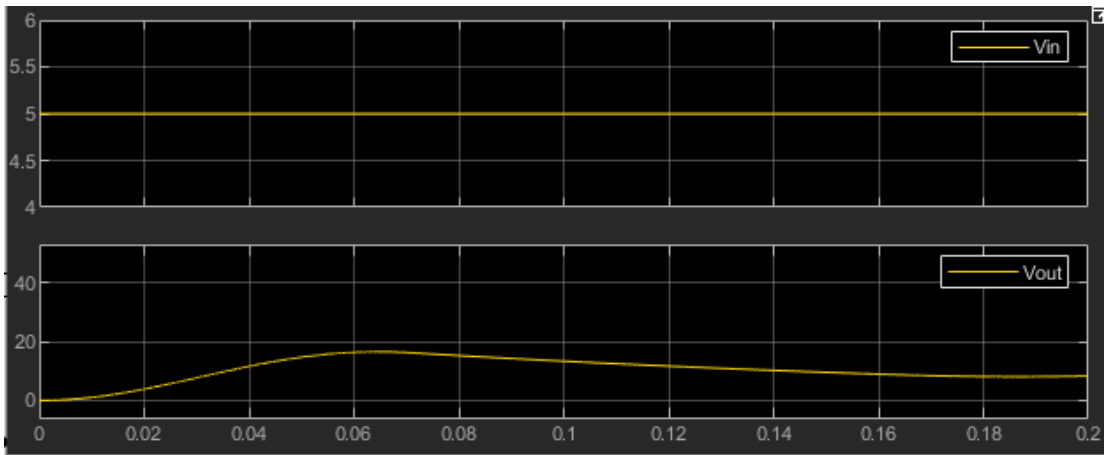
D=0.3



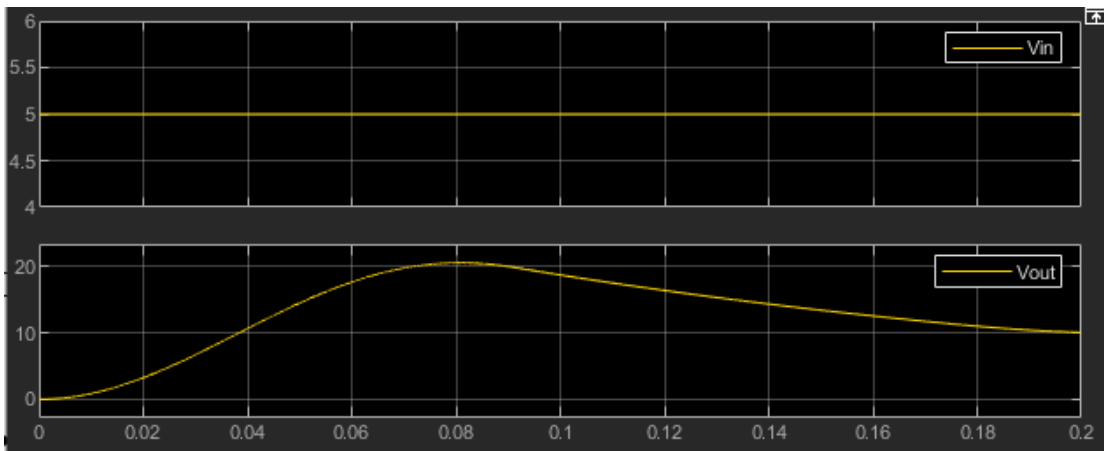
D=0.4



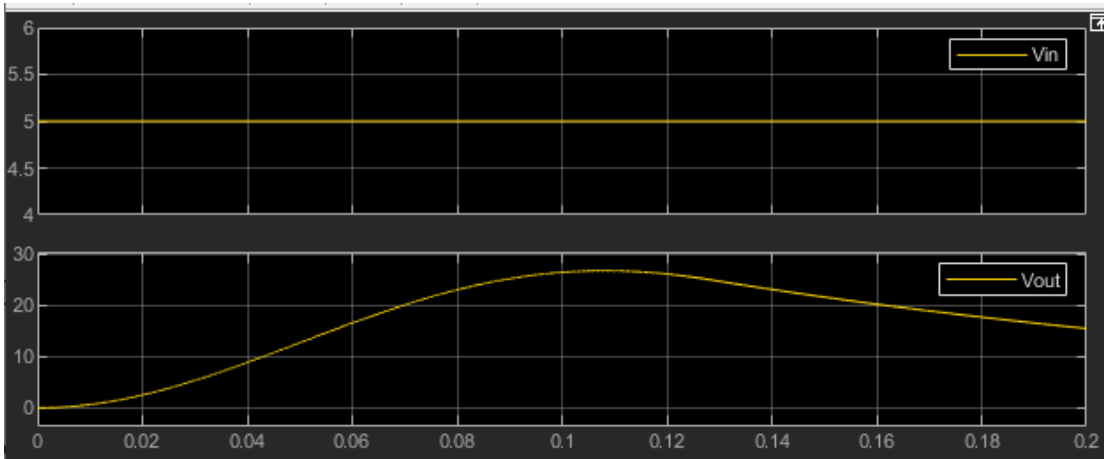
D=0.5



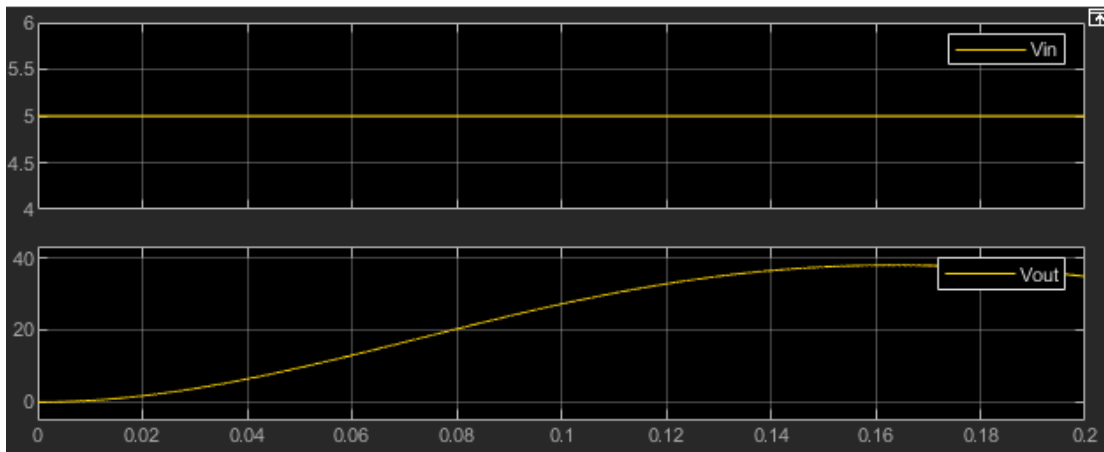
$D=0.6$



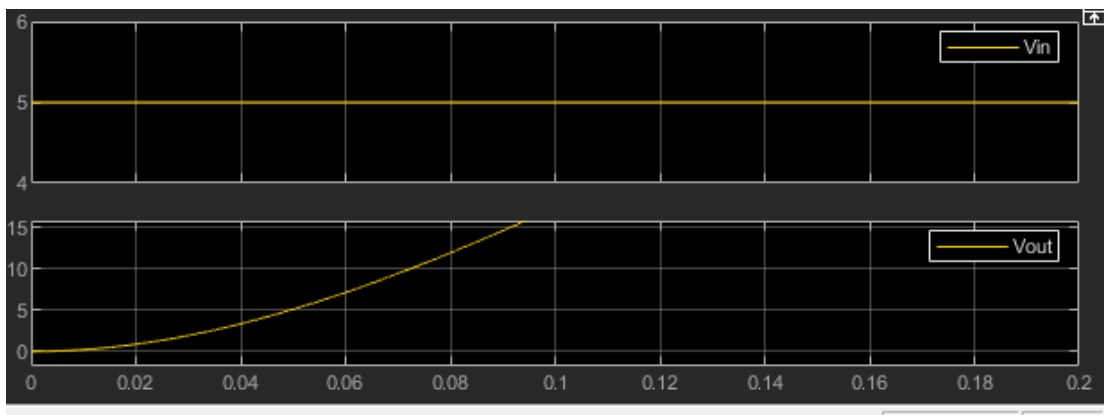
$D=0.7$



$D=0.8$



$D=0.9$



The graph shows how the average output voltage increases as the duty cycle of the boost converter increases. This behavior clearly demonstrates the converter's ability to boost input voltages to higher values, making it indispensable for applications that require boost functionality. Using simulation results, engineers can adjust design parameters to achieve optimal performance characteristics, including minimizing ripple and improving efficiency. This systematic approach ensures that the boost converter effectively meets the stringent operating requirements in a variety of applications.

II.11 Conclusion

In this chapter, we delve into DC-DC converters, tracing their evolution, exploring applications, and discussing key operational considerations. Our focus then shifts to the boost converter, a common type, where we analyze its configuration and intermediate model, providing insights into its operational complexities. We also develop and simulate an equivalent circuit model in Matlab–Simulink, followed by a detailed results analysis.

Chapter III:

BSA and PID-ZN (PID control with Ziegler-Nichols tuning)controller

III.1 Introduction

During the last few decades, many control strategies are proposed for PEM fuel cell power systems. Traditional controllers such as proportional-integral (PI) and proportional-integral derivative (PID) control are widely used in the literature. Thus, Chloé used PID control for a DC–DC boost converter with a fuel cell dynamic model. And Jar used a small signal model with a linearized PEMFC model for controlling the DC–DC converter, given that the parameters of the controller should be changed for any variation in the operating conditions. Authors of used a PI control to keep the PEMFC working in an efficient power point.

The linear control of DC–DC converter is not suitable for PEMFC application. To overcome this issue, many robust control approaches have been developed to cope with nonlinearity and ensure stability.

In Huang demonstrated experimentally that the efficiency of the fuel cell can be improved from 14.67% when using a conventional PID controller to 37% when using a fuzzy controller. However, some oscillations are accrued in the electrical characteristics, which may cause serious life-shortening and severe cell deterioration.

The control process is performed using PID and back stepping which applied to a DC–DC boost converter in order to ensure high and stable output voltage [17].

III.2 Estimating the reference current (I_{ref}) for PEMFC

The goal of this analysis is to establish the reference current, under various operating conditions. As shown in Figure 1, the performance of a Proton Exchange Membrane Fuel Cell (PEMFC) is significantly affected by changes in hydrogen and oxygen pressures, as well as temperature. For this study, the operating hydrogen pressure (P_{H_2}) ranged from 0.01 to 0.6 bar, while the oxygen pressure (P_{O_2}) varied from 0.00022 to 0.0022 bar. The operating temperature (T) was set between 25°C and 50°C.

When (P_{H_2}) and (P_{O_2}) are at their lowest values, 0.01 bar and 0.00022 bar respectively, the PEMFC generates the minimum amount of power. Conversely, when (P_{H_2}) and (P_{O_2}) are

increased to their upper limits, 0.6 *bar* and 0.0022 *bar*, the power output of the PEMFC is maximized, indicating that increased partial pressures lead to enhanced PEMFC performance. This suggests that raising the partial pressures of hydrogen and oxygen can improve PEMFC efficiency.

Additionally, higher operating temperatures can also contribute to increased efficiency, although the impact of temperature changes is less significant compared to that of partial pressures. This indicates that while temperature variations have some influence, the key factors in optimizing PEMFC performance are the partial pressures of hydrogen and oxygen. The latter is constructed using the function given in Equation (1).

The synoptic diagram of this function. It calculates the corresponding .

$I_{ref} = (P)$ [4].

$$f(P) = a_1 * p^4 + a_2 * p^3 + a_3 * p^2 + a_4 * p + a_5 \quad (1)$$

Where: $a_1 = -5041 e^{-010}$, $a_2 = 1191e^{-07}$, $a_3 = -103e^{-04}$, $a_4 = 3943e^{-04}$, $a_5 = 8$

III.3 PI controller

A PI controller calculates an error value as the difference between a measured process variable and a desired set point. The controller attempts to reduce the error by adjusting the process through the use of a manipulated variable.

The error values are calculated via sensor or transducer and compared with desire set point. The detection is in terms of voltage, current, temperature, movement, angle and etc. The PI controller is adjusted manually by setting the value of k_i equal to zero. he value of k_p is manually tuned most likely to Quarter Amplitude Decay (QAD) in order to eliminate any error between the set-point and process variable instantly.

The PI controller will ensure the boost converter deliver a sufficient amount of voltage to the load. By increasing the value of k_i the system until the offset, it will decrease the rise time of the system. However, the system will become unstable and the overshoot will be increased. The value of k_i must be adjusted in certain amount to make sure the system endure the

overshoot while decreasing the settling time and keeping the stability. The derivation of the PI controller is obtained as follow[18]:

$$u(t) = k_p(t) + k_i \int \in (t)dt \quad (2)$$

III.4 PID controller

A proportional integral and derivative (*PID*) controller is considered as the most widely studied and used in both academics and industries due to its simplicity and robustness. The *PID* controller is the aggregates of the three sub-control units, the proportional, integral and derivative control modes. The effective control signal (t) by a *PID* controller in Laplace domain is given by Eq (3) [19].

$$u(t) = k_p \in (t) + k_i \int_0^t \in (t)dt + k_d \frac{d\in(t)}{dt} \quad (3)$$

The relationship of Eq. (4) is the continuous s-domain transfer function:

$$C(s) = k_p + \frac{k_i}{s} + k_d s \quad (4)$$

Where, k_p , k_i and k_d are the proportional gain, integral gain and derivative gain respectively, T_i is the integral time constant and T_d derivative time constant.

PID controllers are designed using five different tuning methods in order to improve the converter transient response and eliminate steady state error.

The procedures for each tuning methods:

- Ziegler-Nichol Frequency Domain Method (ZN-FDM)
- Modified Ziegler-Nichol (MZN)
- Damped Oscillation Method (DOM)
- Tyreus-Luyben Tuning Method (TLM)
- Good Gain Method (GGM)

We will focus on the method [19].

III.5 Ziegler-Nichol frequency domain method(ZN-FDM)

The Ziegler-Nichole frequency method was proposed by Ziegler and Nichole in the 1942 based on sustained oscillation of the system response. The closed-loop system under proportional controller (K_p) is driven to critically stable state by increasing the proportional gain with integral time constant (T_i) set ∞ and derivative constant (T_d) set to 0 . The corresponding gain and period at this point are referred to as ultimate gain K_u and ultimate period p_u [19]. The proportional gain k_p integral (T_i) and derivative constants (T_d) for the PID controller are using the Ziegler-Nichol tuning parameters in Table 5

Table 4: Ziegler-Nichol PID tuning parameters

Type of Controller	k_p	T_i	T_d
P	$0.5K_u$	∞	0
PI	$0.45K_u$	$0.8p_u$	0
PID	$0.6K_u$	$0.5p_u$	$0.125p_u$

III.6 Back stepping

Control theory, back stepping is a technique developed circa 1990 by PetarV. Kokotovic and others for designing stabilizing controls for a special class of nonlinear dynamical systems. These systems are built from subsystems that radiate out from an irreducible subsystem that can be stabilized using some other method. Because of this recursive structure, the designer can start the design process at the known-stable system and "back out" new controllers that progressively stabilize each outer subsystem. The process terminates when the final external control is reached. Hence, this process is known as back stepping [20]. It is well known by its robustness against modeling inaccuracies and system parameter fluctuations. In this work back stepping is a nonlinear control solution that operates according to the nonlinearity of the boost converter [4]

III.6.1 Implementation of the back stepping algorithm

Once the maximum power current I_{ref} is estimated, an algorithm is used to minimize the difference between the desired I_{ref} set point and the actual current measured by the PEMFC (represented by variable x_1). This x_1 -force backtracking algorithm is specifically designed to achieve the most accurate tracking of the I_{ref} value [4].

Step1: Defining the Tracking Current Error

$$\varepsilon_1 = x_1 - I_{ref} \quad (5)$$

Using state–space averaging method dc-dc boost converter can be modelled as [4]:

Where:

$$\mathbf{x} = \begin{bmatrix} x_1 \\ x_2 \end{bmatrix} \quad (6)$$

$$\dot{\mathbf{x}}_1 = -(\mathbf{1} - \mathbf{u}) \left(\frac{1}{L}\right) \mathbf{x}_2 + \left(\frac{V_{in}}{L}\right) \quad (7)$$

$$\dot{\mathbf{x}}_2 = -(\mathbf{1} - \mathbf{u}) \left(\frac{1}{C}\right) \mathbf{x}_1 - \left(\frac{1}{CR}\right) \mathbf{x}_2 \quad (8)$$

Where, equation variables are as labelled. $\mathbf{x}_1 = iL$ is current from the fuel cell input. V_{in} To the boost converter and $\mathbf{x}_2 = V_{out}$ is its output to load voltage. In order to achieve the tracking goal, the $\boldsymbol{\varepsilon}_1$ is needed to fade. So, ε dynamics must be Clearly determined. By placing the equation (5) in the equation (7), time derivative of ε_1 written as [4]:

$$\dot{\boldsymbol{\varepsilon}}_1 = -(\mathbf{1} - \mathbf{u}) \left(\frac{1}{L}\right) \mathbf{x}_2 + \left(\frac{V_{in}}{L}\right) - I_{ref} \quad (9)$$

The Lyapunov functions elected as

$$V_1 = \frac{1}{2} \boldsymbol{\varepsilon}_1^2 \quad (10)$$

Where the quantity $\left(\frac{1}{L}\right) \mathbf{x}_2$ is virtual variable. In order to stabilize the virtual error $\boldsymbol{\varepsilon}_1$, The Lyapunov function V_1 is considered:

Using the above equations, the time derivative \dot{V}_1 can be represented as

$$\dot{V}_1 = \dot{\boldsymbol{\varepsilon}}_1 \boldsymbol{\varepsilon}_1 = \boldsymbol{\varepsilon}_1 \left(-(\mathbf{1} - \mathbf{u}) \left(\frac{1}{L}\right) \mathbf{x}_2 + \left(\frac{V_{in}}{L}\right) - I_{ref} \right) \quad (11)$$

$(\boldsymbol{\varepsilon}_1 = \mathbf{0})$ if $\left(\frac{1}{L}\right) \mathbf{x}_2 = \mathbf{W}$, where the stabilization function \mathbf{W} is defined by the equation:

$$(\mathbf{1} - \mathbf{u}) \left(\frac{1}{L}\right) \mathbf{x}_2 = \left(\frac{V_{in}}{L}\right) - I_{ref}$$

$$\mathbf{w} = \left(\frac{1}{L}\right) \mathbf{x}_2 = \left[\alpha \boldsymbol{\varepsilon}_1 + \left(\frac{V_{in}}{L}\right) - \dot{\mathbf{I}}_{ref} \right] \frac{1}{(1-u)} \quad (12)$$

Where the α is a positive fixed factor and $\left(\frac{1}{L}\right) \mathbf{x}_2$ is a virtual variable and not an actual input of the control unit, these conditions tracking error variable $\boldsymbol{\varepsilon}_2$ will be given the equation):

$$\boldsymbol{\varepsilon}_2 = \left(\frac{1}{L}\right) \mathbf{x}_2 - \mathbf{w} \quad (13)$$

Using equations (12) and (13), the time derivative equation for $\dot{\boldsymbol{\varepsilon}}_1$ can be written as follows:

$$\dot{\boldsymbol{\varepsilon}}_1 = -\alpha \boldsymbol{\varepsilon}_1 - (1-u) \boldsymbol{\varepsilon}_2 \quad (14)$$

And from him: the time derivative $\dot{\mathbf{V}}_1$ it is written as follows

$$\dot{\mathbf{V}}_1 = -\alpha \boldsymbol{\varepsilon}_1^2 - (1-u) \boldsymbol{\varepsilon}_1 \boldsymbol{\varepsilon}_2 \quad (15)$$

Step2: The goal of this step is to ensure that errors ($\boldsymbol{\varepsilon}_1, \boldsymbol{\varepsilon}_2$) first be determined. Using equations (5),(7),(12) and (14), the time derivative of $\boldsymbol{\varepsilon}_2$ can be obtained as:

$$\dot{\boldsymbol{\varepsilon}}_2 = \frac{\dot{u}}{(1-u)} \mathbf{w} + \boldsymbol{\beta} \quad (16)$$

Where

$$\boldsymbol{\beta} = \frac{1}{(1-u)} \left(\alpha^2 \boldsymbol{\varepsilon}_1 + (1-u) \alpha \boldsymbol{\varepsilon}_1 - \frac{\dot{V}_{stak}}{L} - \ddot{\mathbf{I}}_{ref} \right) + \frac{1}{L} \left(\frac{(1-u)}{C} \right) \mathbf{x}_1 - \frac{1}{RC} \mathbf{x}_2 \quad (17)$$

In order to obtain a stabilizing control law V for the whole system, the following Lyapunov function candidate is proposed:

$$V = V_1 + \frac{1}{2}\epsilon_2^2 = \frac{1}{2}\epsilon_1^2 + \frac{1}{2}\epsilon_2^2 \quad (18)$$

Combining the two equations(15)and(16)we get

$$\dot{V} = \dot{V}_1 + \epsilon_1\epsilon_2 \quad (19)$$

$$\dot{V} = -\alpha\epsilon_1^2 + \epsilon_2(\epsilon_2 - (1 - u)\epsilon_1) \quad (20)$$

It can be easily determined that the global asymptotic stability of the equilibrium

$(\epsilon_1; \epsilon_2) = (0; 0)$ is achieved only if the time derivative of the error variable ϵ_2 is chosen as

$$\dot{\epsilon}_2 = -\alpha\epsilon_2 + (1 - u)\epsilon_1 \quad (21)$$

Where δ is a positive design parameter. Finally, by combining Equations (16) and (21), the following control law can be obtained:

$$\dot{u} = \frac{(1-u)}{w}(\delta\epsilon_2 - (1 - u)\epsilon_1 + \beta) \quad (22)$$

Using the above equations, the implementation of the back stepping algorithm in the Matlab–Simulink environment is presented by Figure

The presented curves show the performance of a proton exchange membrane fuel cell (PEMFC) under BSA and PID-ZN (PID with Ziegler-Nichols tuning) control strategies.

Fuel cell current (IFC) versus time comparison of BSA and PID-ZN:

- Both control strategies succeed in raising the current to the desired level quickly, with minor differences in response.
- The BSA control shows a more stable steady-state behavior compared to PID-ZN, which is especially noticeable around the 30 s mark where PID-ZN has small but noticeable fluctuations.

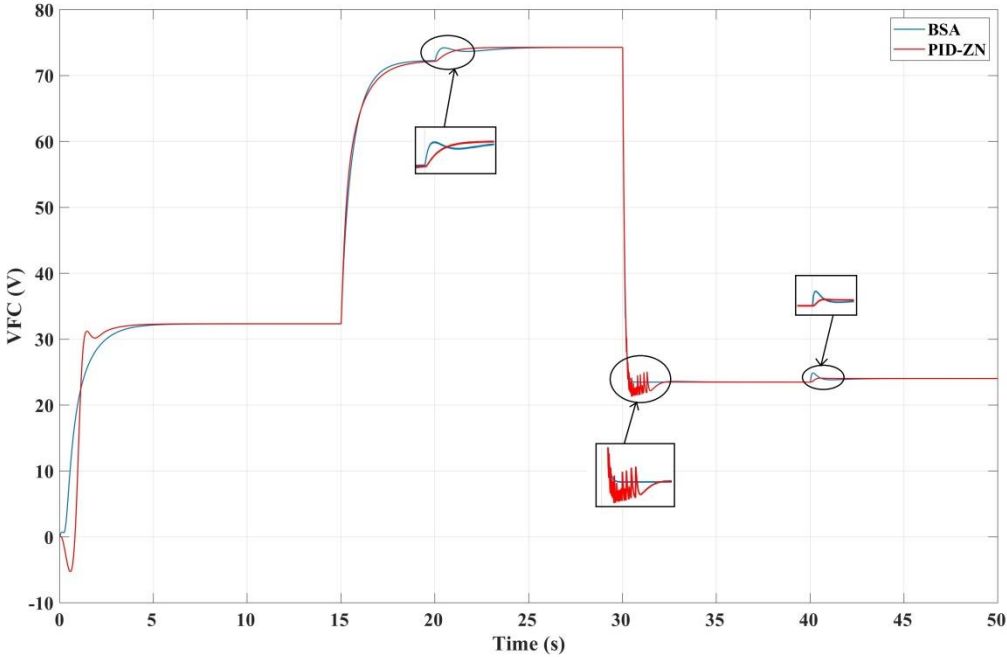


Figure 26: a proton exchange membrane fuel cell (PEMFC) under BSA and PID-ZN (PID with Ziegler-Nichols tuning) control strategies: Fuel cell voltage (VFC) versus time

Fuel cell voltage (VFC) versus time comparison of BSA and PID-ZN:

- Both controllers are able to track voltage changes effectively, but BSA shows a better response, especially during voltage setpoint changes around the 25 s mark.

- PID-ZN shows larger overshoots and more pronounced oscillations compared to BSA, indicating that BSA has better voltage regulation capability and faster settling time.

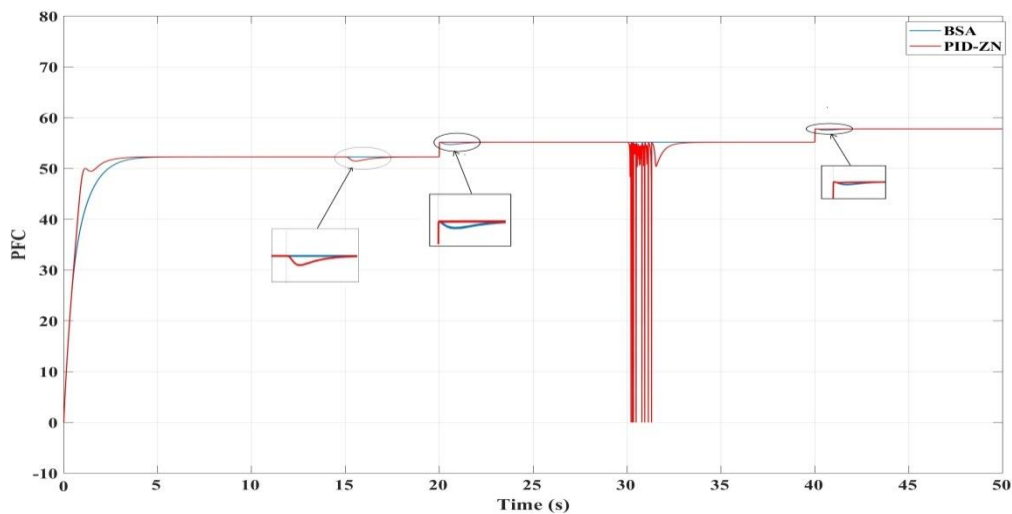


Figure 27: a proton exchange membrane fuel cell (PEMFC) under BSA and PID-ZN (PID with Ziegler-Nichols tuning) control strategies: Fuel Cell (PFC) Power vs. Time

Fuel Cell (PFC) Power vs. Time comparison between BSA and PID-ZN:

- Both control strategies ensure that the power output is tracked until the desired power is obtained, but again, BSA shows superior performance in terms of stability and response time.
- PID-ZN controller shows noticeable oscillations and instability around the 30 second mark, while BSA controller maintains smoother power output with minimal fluctuations.

The BSA control strategy provides better performance in terms of stability, response time and control accuracy for PEMFC systems, making it a recommended approach compared to the conventional PID-ZN method.

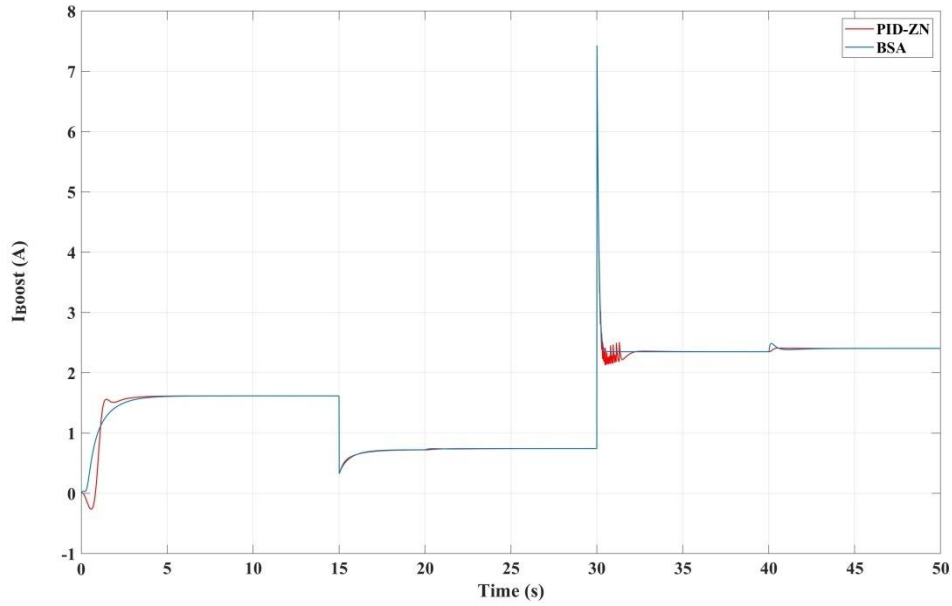


Figure 28: the performance of a DC-DC boost converter using two different control methods: BSA and PID-ZN (PID control with Ziegler-Nichols tuning): Input Current (I_{Boost}) vs. Time (Seconds)

- This graph shows the input current variation over time.
- Both methods (PID-ZN in red and BSA in blue) appear to follow similar trends, but the PID-ZN method shows more fluctuations, especially around the 30-second mark.
- The BSA method appears to provide a more stable input current.

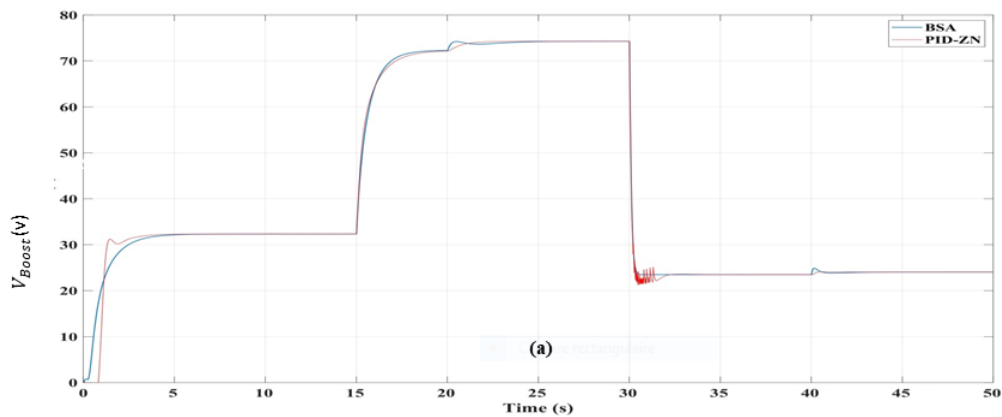


Figure 29: the performance of a DC-DC boost converter using two different control methods: BSA and PID-ZN (PID control with Ziegler-Nichols tuning): Boost voltage (V_{Boost}) versus time (sec)

- This graph shows the boost voltage over time.
- Both methods achieve similar voltage levels, but the BSA method reaches the desired voltage level more smoothly compared to the BSA method. PID-ZN, which shows jitter around 30 seconds.

The BSA method appears to provide more stable and smooth control of the DC-DC boost converter compared to the PID-ZN method, which exhibits larger jitter and transient shifts.

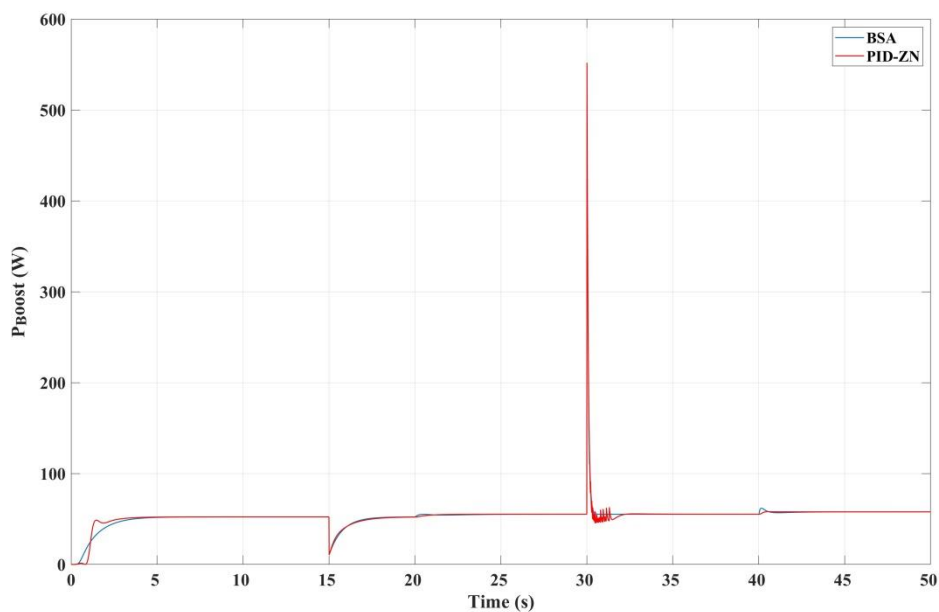


Figure 30: the performance of a DC-DC boost converter using two different control methods: BSA and PID-ZN (PID control with Ziegler-Nichols tuning): Output Power (P_{Boost}) vs. Time (Seconds)

- This graph shows the output power variation over time.
- The red line represents the PID-ZN method and the blue line represents the BSA method.
- The PID-ZN method shows a large peak in output power after about 30 seconds, which could be a transient response or instability.
- The BSA method appears to have a more stable and controlled output without large spikes.

III.8 Conclusion

This chapter examines various control methodologies for managing PEMFC systems, emphasizing the estimation of reference current for optimal performance. We discuss prominent strategies such as PI and PID controllers, along with their principles and adjustment procedures. Notably, we highlight the effectiveness of PID-ZN and Back-Stepping techniques in achieving robust control within PEMFC systems. An equivalent circuit model is developed and simulated in Matlab–Simulink, with comprehensive results analysis.

General conclusion:

In today's era, simulators play an increasingly vital role in many studies due to their availability, flexibility and scalability. With the global focus on reducing CO₂ emissions through international electricity generation strategies, a great deal of attention has been directed towards fuel cells (FC) as a green energy solution. Our project focuses on the design, control and simulation of a fuel cell simulator, which involves several key steps:

- The initial stage involves the selection of the FC type, with our preference being for PEM-FC due to its well-studied characteristics.

We start modeling the chosen PEM-FC type. Here, a great deal of emphasis is placed on the integration of a DC-DC boost converter, which acts as the power component of the FC simulator. This stage also includes the installation of a proportional-integral-derivative (PID) controller and a back-step, whose task is to track the voltage reference of the PEM-FC model.

The PEM-FC simulator was simulated within a MATLAB/SIMULINK environment.

The obtained results proved and confirmed our choice of FC, DC-DC converter and BAS controller in terms of tracking FC behavior, response time and system robustness.

Through this project there were many benefits in the academic career. From another perspective, it is proposed in the future to upgrade to experimental work in order to verify the results obtained.

Bibliography

- [1]:Dalila Hidouri .Rym Marouani .Adnen Cherif . (2023 , November 21). Modeling and Simulation of a Renewable Energy PV/PEM with Green Hydrogen Storage . p. 12543.
- [2]: Ilhan Kocaarslan.Sude Kart. Naci Genc.Hasan Uzmus. (2019, November 11). Design and application of PEM fuel cell-based cascade boost converter. p. 1322.
- [3]:Yuri B. Shtessel, Senior Member, IEEE and Roshini S. Ashok . (December 12-15, 2011). PEM Fuel Cell/ DC-DC Boost Power Converter System Control Via Traditional and Higher Order Sliding Modes . *n Decision and Control and European Control Conference (CDC-ECC)Orlando, FL* (p. 8261). USA.
- [4]:Mohamed Derbeli.Oscar Barambones.Lassaad Sbita . (2018, December 1). A Robust Maximum Power Point Tracking Control Method for a PEM Fuel Cell Power System. p. 2 of 20.
- [5]:Sharjeel Ashraf Ansari .Mustafa Khalid .Khurram Kama.Tahir Abdul Hussain Ratlamwala.Ghulam Hussain.Mohammed Alkahtani. (January 2021, January 25). Modeling and Simulation of a Proton Exchange Membrane Fuel Cell Alongside a Waste Heat Recovery System Based on theOrganic Rankine Cycle in MATLAB/SIMULINK Environment. p. 1and2 of 21.
- [6]:Magsud Hasanov. Philipp Kuehne. (2019, July 15). Review of Components and Materials for Proton Exchange Membrane Unitized Reversible Fuel Cells.
- [7]:Dallia Ali/ Researcher.Daniel D. Aklil-D'Halluin/Managing Director. (25-28 March 2011). Modeling a Proton Exchange Membrane (PEM) Fuel Cell System as a hybrid power supply for standalone applications. *Asia-Pacific powerand energy engineering* <https://doi.org/10.1109/APPEEC.2011.5749114> : Wuhan, China.
- [8]: (n.d.). Retrieved from ENERGY CARRIERS AND CONVERSION SYSTEMS – Vol. II - Fuel Cell Systems - Akifusa Hagiwara

- [9]: Tarek Berghout, Mohamed Benbouzid, Toufik Bentrchia, Yassine Amirat, Leïla-Hayet Mouss. (2022, July 21). Exposing Deep Representations to a Recurrent Expansion with Multiple Repeats for Fuel Cells Time Series Prognosis. p. 2 of 12.
- [10]: A. Baroutaji, J. G. Carton, J. Stokes, A. G. Olabi. (2014, September 6). Design and development of proton exchange membrane fuel cell using open pore cellular foam as flow plate material. *Journal of Energy Challenges and Mechanics*, 96.
- [11]: (n.d.). Retrieved from <https://dbrau.ac.in/wp-content/uploads/2023/05/CP-Fuel-Cell.pdf>
- [12]: M. T. Outeiro, R. Chibante, A. S. Carvalho, A.T. de Almeida. (2007, November 11-15). DYNAMIC MODELING AND SIMULATION OF AN OPTIMIZED PROTON EXCHANGE MEMBRANE FUEL CELL SYSTEM . p. 2.
- [13]: (n.d.). Retrieved from https://www.academia.edu/8335984/A_Comprehensive_Review_of_Fuel_Cell_and_its_Types_1_4
- [14]: Mohammed Yousri Silaa .Oscar Barambones .José Antonio Cortajarena. Patxi Alkorta. Aissa Bencherif. (2023, September 16). PEMFC Current Control Using a Novel Compound Controller Enhanced by the Black Widow Algorithm: A Comprehensive Simulation Study. pp. 4,5 and 6 of 23.
- [15]: Abdul Fathah (109EE0612). (June-2013). *Design of a Boost Converter*. NATIONAL INSTITUTE OF TECHNOLOGY, Department of Electrical Engineering. ROURKELA ODISHA, INDIA-769008.
- [16]: MEHEDI HASAN TUSHAR ID-09221205. (n.d.). *COMPARATIVE STUDY ON DC-DC CONVERTERS*. THESIS FINAL SEMESTER.
- [17]: Liping Fan. Xianyang Ma. (2022). Maximum power point tracking of PEMFC based on hybrid artificial bee colony algorithm with fuzzy control.
- [18]: Afarulrazi Abu Bakar. Wahyu Mulyo Utomo. Taufik Taufik. Shamsul Aizam. (2015, January). DC/DC boost converter with PI controller using Real-Time Interface.

- [19]: Oladimeji Ibrahim.Zaihar Yahaya's.Nordin Saad. (2016, June). PID Controller Response to Set-Point Change in DC-DC Converter Control.
- [20]: Yasir Khudhair Abbas.Assist. Prof. Dr. Shibly Ahmed Al-Samarraie. (2012-2013). *Backstepping Control Design Lab.* Control Engineering.
<https://uotechnology.edu.iq/dep>: Iraq-Baghdad.